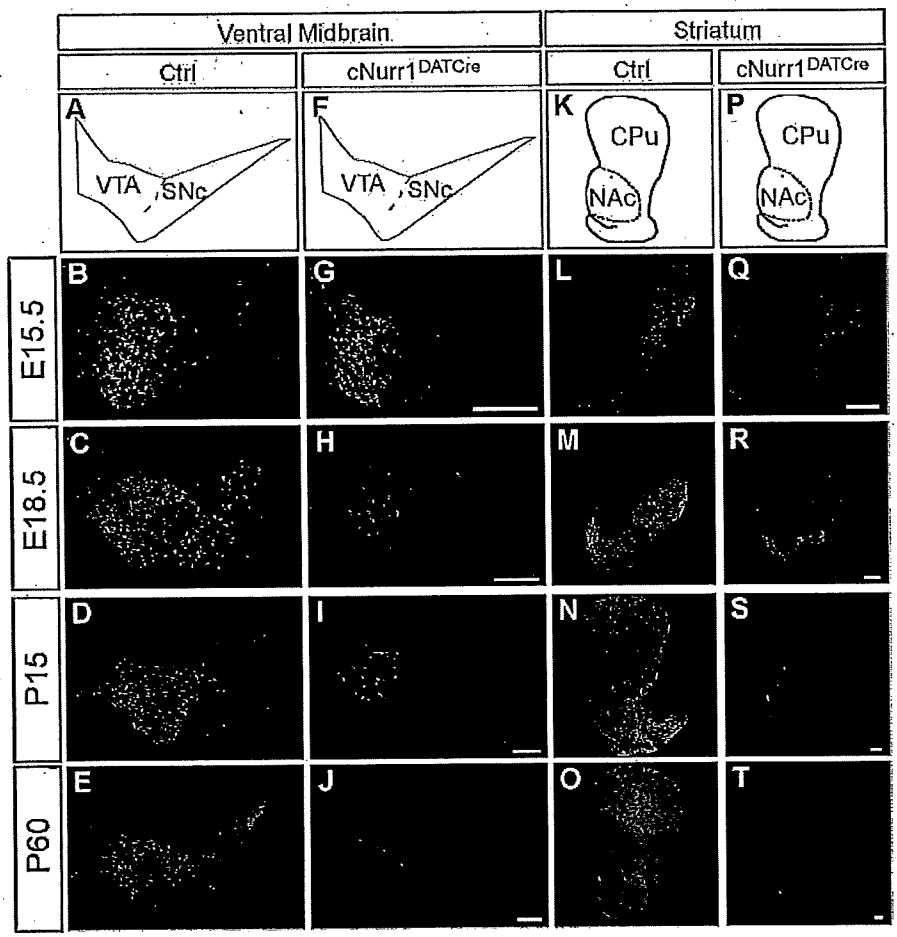

Figure 1. TH is progressively lost in both the ventral midbrain and striatum of *cNurr1*^{DATCre} mice. ***A–T***, Confocal microscopy showing TH immunohistochemistry in control (ctrl) and *cNurr1*^{DATCre} mice as indicated. ***A–J***, Sections were analyzed at the levels of ventral midbrain (as indicated in ***A*** and ***F***) and in the striatum (as indicated in ***K*** and ***P***). TH immunofluorescence was analyzed at both embryonal and postnatal stages as indicated. Results demonstrate a progressive loss of TH immunoreactivity in the ventral midbrain. Note that TH immunoreactivity was more drastically downregulated at more lateral regions compared with the prospective medial VTA. ***K–T***, TH immunoreactivity in the striatum. In *cNurr1*^{DATCre} mice, TH was lost in the CPu and diminished in the NAc. Scale bars, 250 μm.

modifications. Briefly, 25 μl of each sample were injected by a cooled autosampler (Midas) into an ESA Coulochem III coupled with an electrochemical detector. The mobile phase (5 g/L sodium acetate, 30 mg/L Na2-EDTA, 100 mg/L octane-sulfonic acid, and 10% methanol, pH 4.2) was delivered at a flow rate of 500 μl/min to a reverse-phase C18 column (4.6 mm diameter, 150 mm).

Fluorogold retrograde tracing. Animals received one unilateral stereotaxic injection in the right striatum using a 5 μl Hamilton microsyringe (22 gauge steel cannula) filled with the retrograde tracer Fluorogold (hydroxystilbamidine, 4%, Biotium). The animals were anesthetized with isoflurane, 0.5 μl was injected during 1 min, and the cannula was left in place for an additional 2 min before slowly being retracted. The anteroposterior and mediolateral coordinates from bregma were 0.27 and −2.10 mm, respectively, and the dorsoventral coordinates from the dura were −2.60 mm. Animals were killed 4 d after injection, and the brains were isolated. Fresh-frozen sections (14 μm) were cut with a cryostat and examined under a epifluorescence microscope (Eclipse E1000K; Nikon) coupled to an RTke spot camera.

Open-field test. This test was used to monitor overall activity and rearing behavior. The open field consisted of a white plastic box (55 × 35 × 30 cm) with lines (squares of 7 × 35 cm) painted on its floor. The animals were put in the center of the box, habituated for 10 min, and filmed 15 min thereafter while rearing was scored. The video recordings were used to measure the number of lines crossed during the monitoring period. A line crossing was counted when the mouse moved its whole body from one square to another.

Stepping test. Forelimb akinesia was monitored in a modified version of the stepping test, as described previously for rats (Schallert et al., 1992; Kirik et al., 1998). The test was performed three times daily over 3 consecutive days. In this test, the mouse was held firmly by the experimenter with both hindlimbs and one forelimb immobilized, and the mouse was passively moved with the free limb contacting a table surface. The number of adjusting steps, performed by the free forelimb when moved in the forehand and backhand directions, over a distance of 30 cm, was recorded. Results are presented as data collected on the third testing day.

Results

Selective *Nurr1* ablation in late developing mDA neurons

A mouse strain containing a *Nurr1* allele for conditional gene ablation was generated by insertion of two loxP sequences in the second and third introns so that the coding sequence, including the first coding exon 3, is excised by Cre-mediated recombination (supplemental Fig. 1, available at www.jneurosci.org as supplemental material). To analyze the consequences of *Nurr1* ablation at late stages of mDA neuron development, we crossed floxed *Nurr1* mice with mice carrying *Cre* inserted in the locus of the *DAT* gene (Ekstrand et al., 2007). Crosses generated *Nurr1* mice that were homozygous for the conditional targeted *Nurr1* allele and heterozygous for the *DAT–Cre* allele (*Nurr1*$^{L2/L2}$;*DAT*$^{Cre/wt}$; hereafter referred to as *cNurr1*^{DATCre} mice). Littermates of genotype *Nurr1*$^{L2/L2}$; *DAT*$^{wt/wt}$ or *Nurr1*$^{w/w}$;*DAT*$^{Cre/wt}$ were used as controls. Although we cannot exclude that a small number of cells escape Nurr1 gene deletion, immunohistochemistry using an antibody against Nurr1 showed that *DAT–Cre*-mediated *Nurr1* ablation resulted in the expected delayed loss of Nurr1 expression in mDA neurons beginning from approximately E13.5 and becomes essentially complete at E15.5 (supplemental Fig. 2, available at www.jneurosci.org as supplemental material). At this stage of normal development, cells express pan-neuronal properties as well as many mDA neuron markers, and axons are growing toward the developing striatum (Smidt and Burbach, 2007).

cNurr1^{DATCre} mice were born at the expected Mendelian frequency of ~25% (of a total $n = 159$); however, *cNurr1*^{DATCre} mice were less active than controls and did not survive beyond 3 weeks after birth. If litters were allowed to remain with their mothers after weaning, perinatal death was avoided in ~50% of *cNurr1*^{DATCre} pups. These surviving mice were, however, ~40% smaller than controls at the age of 2 months (supplemental Fig. 3, available at www.jneurosci.org as supplemental material). Although no significant change in spontaneous light-phase locomotor activity could be observed in adult *cNurr1*^{DATCre} mice, rearing was dramatically decreased (supplemental Fig. 3, avail-

able at www.jneurosci.org as supplemental material). L-DOPA treatment of mutant mice did not improve viability and did not induce any weight gain. Instead, *cNurr1*^{DATCre} mice display a pronounced and severe hypersensitivity to L-DOPA treatment characterized by an acute phase of hyperactivity and repetitive behaviors (including repetitive gnawing, excessive grooming, and self-injury) in all tested mutant ($n = 9$) but not in any wild-type controls ($n = 7$) (see Materials and Methods). These behaviors resemble those that have been observed in neonatal 6-hydoxydopadmine lesioned rats treated with L-DOPA (Breese et al., 2005). In conclusion, late embryonic mDA neuron-selective *Nurr1* ablation is associated with decreased weight, rearing, and viability, and mice show an altered response to L-DOPA.

Reduced levels of TH and DA in brains of *cNurr1*^{DATCre} mice

The observed abnormalities are consistent with a dopaminergic deficiency. To analyze the possible cellular basis for the phenotype, brain sections from controls and *cNurr1*^{DATCre} mice were analyzed by immunohistochemistry using an antibody against TH (Fig. 1). A progressive loss of TH immunostaining in SNc was observed in the *cNurr1*^{DATCre} mice (Fig. 1*A–J*). TH levels were significantly decreased already at E15.5, soon after Nurr1 is lost, and decreased further until adulthood when only scattered TH-positive neurons could be detected. TH was diminished also within the VTA at later stages, but a significant number of cells remained even in adult animals (Fig. 1*A–J*). These cells were counted in four nonconsecutive sections for each analyzed brain. In adult control VTA, a mean of 74.5 ± 7.1 cells per section were counted in *cNurr1*^{DATCre} mice ($n = 4$) and 499.3 ± 5.2 cells in controls ($n = 3$) (Student's *t* test, 4.4×10^{-7}). TH immunostaining within the caudatus putamen (CPu) was completely lost (Fig. 1*K–T*). However, weak immunoreactivity remained in nucleus accumbens (NAc) innervated preferentially by VTA neurons (Fig. 1*K–T*). We also noted the appearance of ectopic TH-positive cell bodies within the striatal parenchyma in *cNurr1*^{DATCre} mice (supplemental Fig. 4, available at www.jneurosci.org as supplemental material). These cells were more frequent in regions in which striatal TH had been most severely depleted as a consequence of Nurr1 ablation and resemble TH-positive neurons appearing in rodent and primate DA-depletion models (Huot and Parent, 2007). Decreased levels of TH immunostaining were paralleled by decreased DA levels, as measured by HPLC (supplemental Tables 1–3, available at www.jneurosci.org as supplemental material). Striatal DA was dramatically reduced to 14% of controls at P1 in *cNurr1*^{DATCre} mice and was almost completely lost by P60. An increased ratio of HVA to DA at P14 indicated increased turnover of DA in remaining cells at this stage (supplemental Table 2, available at www.jneurosci.org as supplemental material). DA was more severely decreased in CPu compared with NAc (supplemental Table 3, available at www.jneurosci.org as supplemental material). In contrast, 5-HT was significantly increased in both CPu and NAc, consistent with previous findings showing increased serotonergic innervation after striatal DA depletion (Snyder et al., 1986). Thus, a severe neurotransmitter deficiency of the mesostriatal DA system is apparent in *cNurr1*^{DATCre} mice. Together, measurements of TH immunoreactivity and DA levels demonstrate that Nurr1 is critically required for maintaining TH expression and DA synthesis from late stages of mDA neuron differentiation.

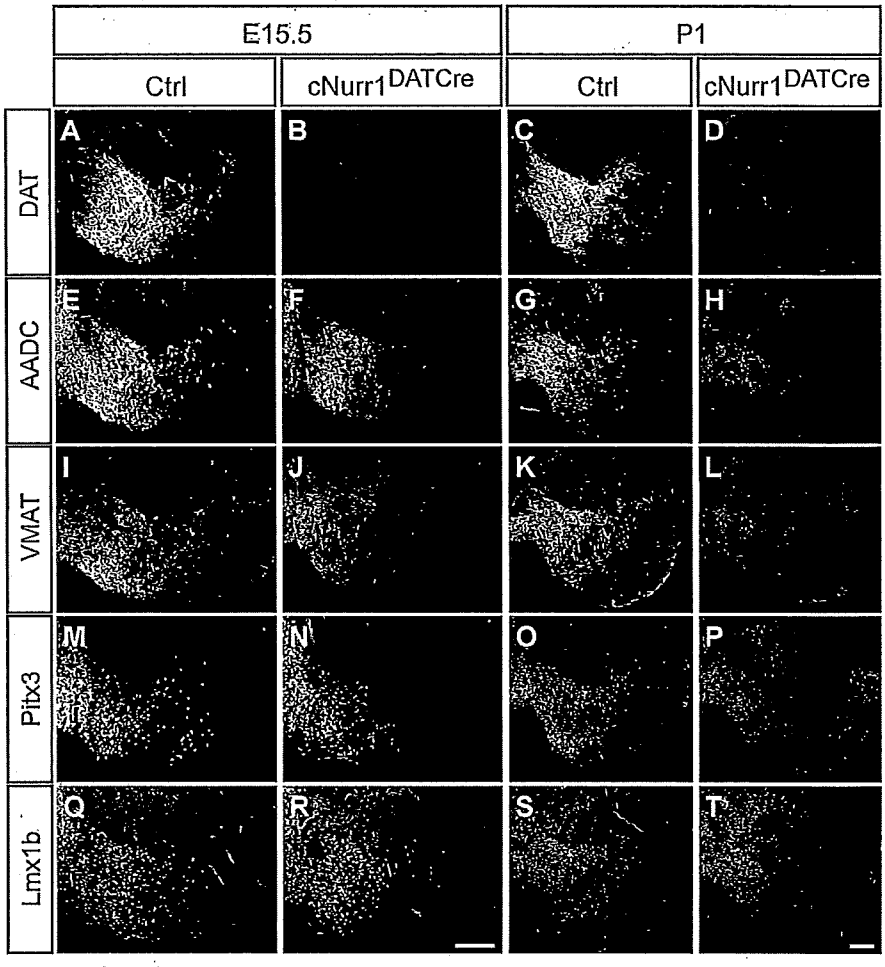

Figure 2. All analyzed mDA neuron markers are lost or diminished in *cNurr1*^{DATCre} mice. ***A–T***, Confocal microscopy showing immunohistochemistry of several different mDA neuron markers in control (ctrl) and in *cNurr1*^{DATCre} mice at E15.5 or at P1, as indicated. The following markers were analyzed: DAT, AADC, VMAT, Pitx3, and Lmx1b. Results show a progressive loss of markers that is more substantial in the lateral SNc, whereas more medial VTA cells are lost more slowly. DAT is completely absent already at E15.5 in *cNurr1*^{DATCre} mice, whereas all other markers are decreased more slowly in this area (compare ***A***, ***B***). Scale bars, 200 μm.

Cellular deficiency within the ventral midbrain of *cNurr1*^{DATCre} mice

To investigate whether the phenotype is a consequence of a more limited disruption of DA synthesis or a more severe cellular deficiency, a number of additional mDA neuron markers were analyzed. All analyzed mDA neuron markers were diminished or absent within SNc in *cNurr1*^{DATCre} mice already at E15.5 (Fig. 2). DAT was completely lost at E15.5 and therefore, consistent with previous data (Sacchetti et al., 1999), stands out as being a likely direct target of Nurr1 (Fig. 2*A–D*). Additional control experiments showed that DAT and other markers, including TH and

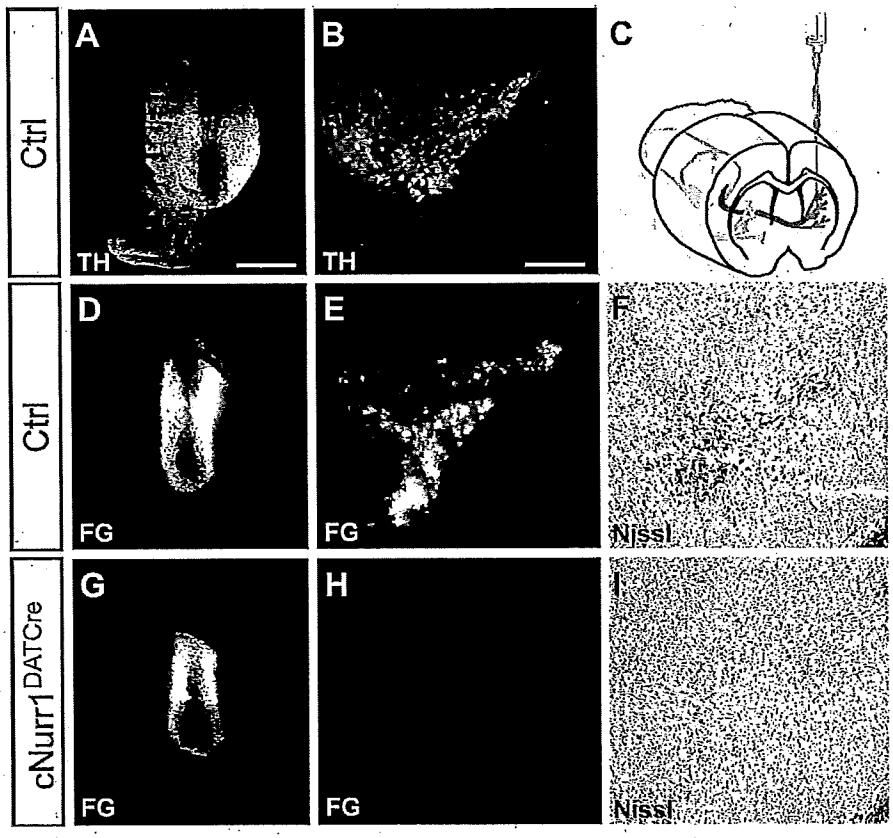

Figure 3. Cell bodies and striatal innervation are lost in *cNurr1*^{DATCre} mice as determined by Fluorogold (FG) retrograde tracing of fibers extending from cell bodies in SNc to the striatum. ***A–C***, After Fluorogold injection, injected into the left striatum in either adult (1.5 months old) control (Ctrl) or *cNurr1*^{DATCre} mice as indicated in ***C***, mice were killed after 4 d and analyzed for TH immunofluorescence in the striatum (***A***) or ventral midbrain (***B***). ***D–I***, Analysis for Fluorogold (FG) or by Nissl staining. Strong Fluorogold staining in both striatum (***D***) and in the ventral midbrain (***E***) was consistently seen in all control (Ctrl) animals ($n = 7$). In contrast, Fluorogold fluorescence was only detected in the striatum (***G***) in *cNurr1*^{DATCre} mice ($n = 5$), indicating that fibers from the SNc (***H***) had been lost in these animals. Moreover, large, densely packed cell bodies are only visualized by Nissl staining in the ventral midbrain of control animals (***F***) but are completely absent from *cNurr1*^{DATCre} mice (***I***). Striatal site of Fluorogold injection is marked by asterisk in ***A***, ***D***, and ***G***. Scale bars: ***A***, ***B***, ***D***, ***E***, ***G***, ***H***, 1 μm; ***F***, ***I***, 1200 μm.

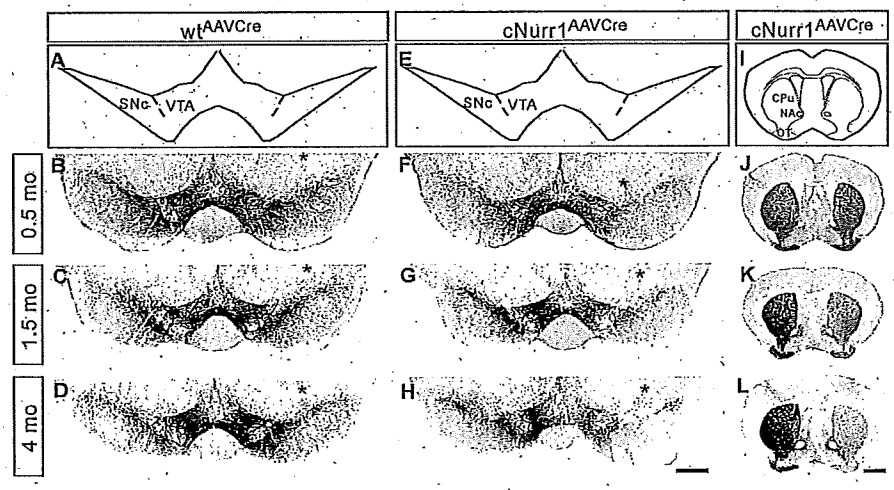

Figure 4. TH expression in both the ventral midbrain and striatum is progressively lost in the injected, but not non-injected, side of *cNurr1*^{AAVCre} mice. ***A–H***, Sections from 0.5, 1.5, and 4 month (mo; as indicated) old AAV–Cre-injected controls (*wt*^{AAVCre}) or *cNurr1*^{AAVCre} mice were used for analyses by nonfluorescent DAB TH immunostaining in the ventral midbrain. The analyzed region within the ventral midbrain is schematically illustrated in ***A*** and ***E***. The site of injection, marked by an asterisk in ***B–D*** and ***F–H***, was verified in all animals by high-power magnification microscopy and was identified as a small area of injection-induced necrosis. Results show that TH immunostaining is not drastically altered at 0.5 months but is progressively decreased at 1.5 and 4 months in the injected SNc and VTA. ***I–L***, DAB TH staining at the level of striatum. Analyzed regions are indicated in ***I***. TH staining is progressively decreased at 1.5 and 4 months in the side that is ipsilateral to the side of AAV–Cre injection in *cNurr1*^{AAVCre} mice (***J–L***). OT, Olfactory tubercle. Scale bars: ***A–H***, 600 μm; ***I–L***, 1 mm.

Nurr1, were not visibly decreased in mice heterozygous for the *DAT–Cre* allele (supplemental Fig. 5, available at www.jneurosci.org as supplemental material) (data not shown). In contrast to DAT, AADC, VMAT2, Pitx3, or Lmx1b were not reduced within the most medial ventral midbrain at this early stage and, with the exception of DAT, markers were not completely downregulated at P1 (Fig. 2*E–T*). The progressive loss of markers indicates a severe loss of phenotype within the SNc, whereas cells within the VTA appear more resilient. Importantly, most TH-positive cells within the VTA have lost any detectable expression of DAT, indicating that these cells have not escaped Nurr1 gene targeting (supplemental Fig. 6, available at www.jneurosci.org as supplemental material).

To further assess the extent of a cellular deficiency, striatal target innervation was analyzed by Fluorogold retrograde tracing after injection into the striatum of live 8- to 9-week-old controls and *cNurr1*^{DATCre} mice. Fluorogold was transported into SNc cell bodies of control mice; however, fluorescence was entirely undetected within the SNc of Fluorogold-injected *cNurr1*^{DATCre} mice (Fig. 3, compare *D*, *E* with *G*, *H*). In addition, characteristic large and densely packed TH-immunoreactive mDA neurons within the SNc were virtually absent in *cNurr1*^{DATCre} mice (Fig. 3*I*). In conclusion, Nurr1 ablation in *cNurr1*^{DATCre} mice results in rapid loss of SNc cell bodies; however, scattered VTA neurons remained even in adult *cNurr1*^{DATCre} mice.

Adeno-associated virus–Cre-mediated *Nurr1* ablation in adult mice

In *cNurr1*^{DATCre} mice, *Nurr1* is ablated well before full mDA neuron maturity and before targets in the striatum have become innervated; thus, it remained possible that the phenotype is a consequence of a developmental dysfunction. Therefore, we proceeded to inactivate *Nurr1* specifically in ventral midbrain of adult mice, using an adeno-associated virus (AAV)–Cre vector driven by the neuron-specific synapsin promoter. AAV–Cre was administered by unilateral stereotaxic microinjection above the right SNc. Cre immunohistochemistry and β-galactosidase expression was analyzed after intranigral AAV–Cre injection into reporter mice in which the ROSA26 locus is targeted with a LacZ reporter gene (Soriano, 1999). Results show widespread Cre expression around the site of injection, spreading into both SNc and VTA, and robust recombination of the LacZ reporter construct (supplemental Fig. 7, available at www.jneurosci.org as supple-

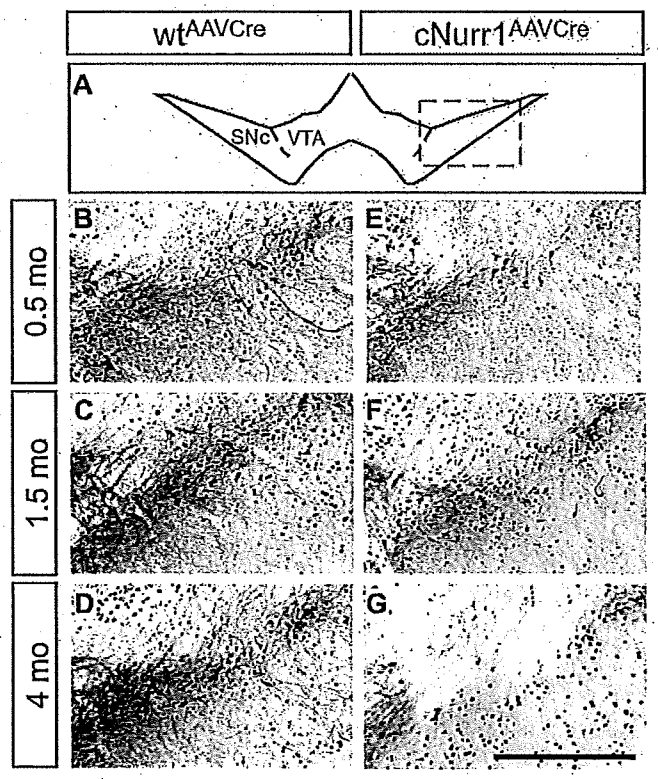

Figure 5. Cre-expressing cells are lost at 4 months within the SNc after Nurr1 ablation. *A*, Higher magnification showing TH by DAB staining (brown) at the level of the injected SNc in wt^{AAVCre} and $cNurr1^{AAVCre}$ mice. The region that has been magnified is boxed in *A*. *B–G*, Adjacent sections were immunostained for Cre (black) and are superimposed on the DAB-stained TH sections in all micrographs. Cre staining is widespread in the area in which mDA neurons are normally localized at 0.5 and 1.5 months (*E*, *F*) but almost completely absent in this area at 4 months (*G*). Scale bar, 500 μm.

mental material). Moreover, except for a small necrotic area around the site of injection, virus administration did not affect tissue morphology, expression of mDA neuron markers, or microglia activation (data not shown).

AAV–Cre was unilaterally injected above the SNc of adult mice homozygous for the floxed *Nurr1* allele to generate adult conditional gene-targeted mice ($cNurr1^{AAVCre}$) or into wild-type control mice (wt^{AAVCre}). In addition, a vector encoding the green fluorescent protein (GFP) driven by the synapsin promoter (AAV–GFP) was injected in mice homozygous for the floxed *Nurr1* allele ($cNurr1^{AAV-GFP}$ mice) to ensure that the floxed animals are not more sensitive to nonspecific toxicity induced by AAV transduction. Histological analyses were performed from animals killed at 0.5, 1.5, and 4 months after injection.

Reduction of TH and DA in adult *Nurr1*-ablated mice

TH immunohistochemistry at the level of the ventral midbrain was analyzed to assess the consequences of adult *Nurr1* ablation. Within SNc, TH immunoreactivity was unaffected at 0.5 months but was progressively reduced at 1.5 and 4 months in the injected SNc in $cNurr1^{AAVCre}$ mice (Fig. 4*E–H*). In contrast, TH immunoreactivity was unaffected in SNc of control wt^{AAVCre} and $cNurr1^{AAV-GFP}$ mice (Fig. 4*A–D*) (data not shown). TH was also reduced in the VTA at 1.5 and 4 months; however, at 4 months, the reduction in VTA was less dramatic compared with SNc (Fig. 4*E–H*).

Decreased striatal TH immunoreactivity paralleled the reduction in the ventral midbrain. Thus, although no signs of degenerating striatal TH-stained fibers (swollen axons or dystrophic neurites) were detected, striatal sections ipsilateral to the side of AAV–Cre injection showed clearly reduced TH in $cNurr1^{AAVCre}$ mice but not in controls (wt^{AAVCre} or $cNurr1^{AAV-GFP}$) (Fig. 4*I–L*) (supplemental Fig. 8, available at www.jneurosci.org as supplemental material). Diminished TH immunoreactivity was observed in regions innervated by both SNc and VTA (CPu and NAc, respectively), consistent with the reduced TH immunoreactivity in both SNc and VTA mDA neuron cell bodies. Measurement of DA and metabolites by HPLC from dissected tissue at 4 months confirmed this picture as a significant reduction in DA and DA metabolites noted both within the dorsolateral striatum and in areas mostly innervated by the VTA (cortex and ventromedial striatum) (supplemental Table 4, available at www.jneurosci.org as supplemental material). Thus, TH, DA, and DA metabolites are clearly reduced as a result of adult *Nurr1* ablation.

Loss of mDA neuron characteristics in adult *Nurr1*-ablated mice

To further analyze the fate of *Nurr1*-ablated neurons, cells were counted within the SNc and VTA in $cNurr1^{AAVCre}$ and wt^{AAVCre} mice. Within SNc, the number of TH-positive cells was significantly decreased at 4 months (58.1 ± 8.3 and 95.4 ± 6.3% in the injected vs non-injected sides of $cNurr1^{AAVCre}$ and wt^{AAVCre} mice, respectively; $p = 0.0053$). In contrast, the numbers of TH-positive cells was not significantly reduced within the VTA (104.1 ± 4.7 and 101.6 ± 10.5% in the injected versus non-injected sides of $cNurr1^{AAVCre}$ and wt^{AAVCre} mice, respectively). Also, the numbers of TH-positive cells were not significantly changed in $cNurr1^{AAVCre}$ mice at 1.5 months (data not shown).

To assess the integrity of neurons, cellular analysis was extended by analyzing Cre-immunolabeled sections that were superimposed on adjacent TH-labeled sections (Fig. 5). Notably, in $cNurr1^{AAVCre}$ mice, Cre expression was clearly detected within the area of SNc at both 0.5 and 1.5 months but was lost at 4 months in the region in which mDA neurons should normally be localized (Fig. 5, compare *E–G* with *B–D*). Cre expression is driven by a general neuronal promoter (synapsin), suggesting that loss of Nurr1 may eventually affect some pan-neuronal properties at 4 months after ablation.

Confocal microscopy confirmed the loss of TH at 1.5 and 4 months after Nurr1 ablation and the loss of Cre at 4 months (Fig. 6*A–D*). At 1.5 months, DAT expression was weak but cell bodies were readily identified (Fig. 6*E*,*F* and inset in *F*). DAT staining remained also at 4 months, but, at this stage, high-power magnification indicated that some of the staining appeared confined to fibers and/or dystrophic cells (Fig. 6*G*,*H* and inset in *H*). Nonetheless, at 4 months, most cells with decreased TH stained positive for AADC, showing that not all mDA neuron characteristics were affected (Fig. 7*A–F*). Moreover, VMAT2 is yet another marker that was severely decreased in $cNurr1^{AAVCre}$ mice, but remaining weakly stained cells were positive for the general neuronal marker Hu (Fig. 7*G–L*). The observed changes were not correlated to increased number of apoptotic cells because increased activated Caspase 3 could not be detected (data not shown). Also, we found no evidence for nigral inflammation or α-synucleinopathy because activated microglia and α-synuclein-rich inclusions were not detected at any stage after Nurr1 ablation in $cNurr1^{DATCre}$ mice (data not shown). Finally, TH and DAT expression in VTA was also affected, without any apparent loss of the neuronal marker Hu or any signs of dystrophic cells (supplemental Fig. 9, available at www.jneurosci.org as supplemental material) (data not shown). Thus, Nurr1 ablation results in a

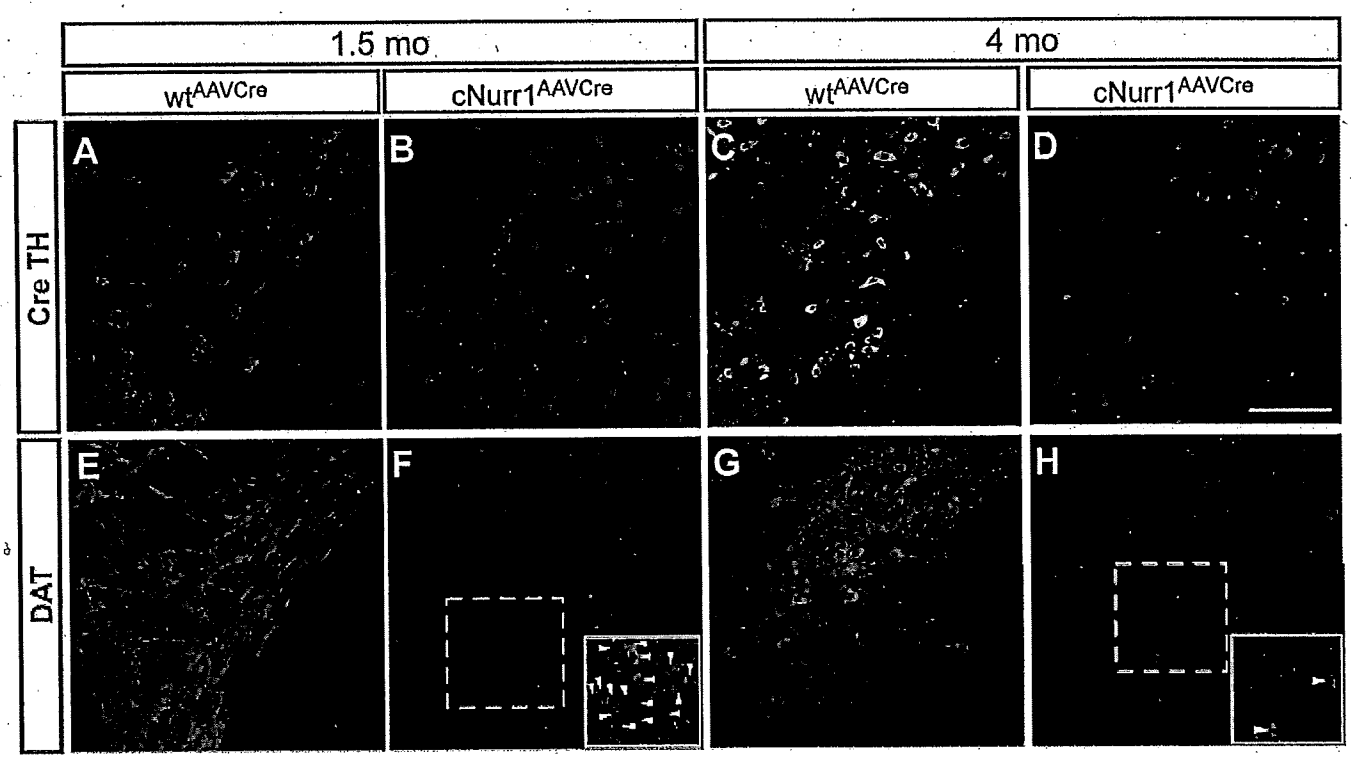

Figure 6. Decreased expression of DAT and signs of dystrophic cells in *cNurr1*^{AAVCre} mice. ***A–H***, Confocal analysis of SNc in *wt*^{AAVCre} and *cNurr1*^{AAVCre} mice at 1.5 and 4 months, as indicated. Confocal images show double staining of Cre (red) and TH (green; ***A–D***) and staining for DAT (green; ***E–H***). Micrographs show that there is a loss of TH and DAT and a progressive loss of synapsin-driven Cre at 4 months. At 4 months, DAT staining appears fragmented and stains scattered fibers, whereas very few intact cell profiles (marked with arrowheads in ***F*** and ***H***) can be identified in *cNurr1*^{AAVCre} mice (compare insets in ***F***, ***H***). Scale bar, 200 μm.

progressive dysfunction characterized by a partial loss of the mDA neuron phenotype. Although we see few signs of neuronal degeneration, we cannot exclude a limited cell loss.

To assess whether the observed dysfunction was paralleled by an altered motor behavior, *cNurr1*^{AAVCre} mice were subjected to a stepping test at 3 and 4 months (Schallert et al., 1992; Kirik et al., 1998). Performance of the left forelimb (i.e., the limb contralateral to the vector injection) was impaired at both time points (Fig. 8). Additional behavioral testing, including amphetamine-induced rotations and a corridor test, indicated that individual mutant animals appeared affected; however, the *Nurr1*-ablated group did not show alterations that were statistically significant (supplemental Fig. 10, available at www.jneurosci.org as supplemental material). Our results demonstrate progressive mDA neuron dysfunction, leading to a more severe deficiency at 3–4 months after *Nurr1* ablation.

Discussion

This study provides definitive evidence that Nurr1 is not only critical for early differentiation but also for the maintenance of functional mDA neurons. Conditional gene targeting at late embryogenesis, when characteristic features of mDA neurons are already apparent, results in a rapid and close to complete mDA neuron loss. Only few TH-positive cells remain within the VTA also in the absence of Nurr1. Removal of Nurr1 leads to a severe dysfunction also in adult mDA neurons. It should be noted that reduction of striatal DA and the behavioral effects after adult ablation most likely underestimate the importance of Nurr1 in the adult brain because AAV injection only transduced a proportion of all mDA neurons in the injected side of treated animals. Thus, these data emphasize the importance of studying developmental mechanisms for elucidating neuron maintenance mechanisms. An analogous example is provided by the glial cell line-derived neurotrophic factor (GDNF). GDNF is known to promote neuronal survival under development, but only recently has conditional gene targeting enabled studies that interrogate the role of GDNF and other factors signaling via Ret for maintenance of midbrain dopamine neurons in the adult brain (Oo et al., 2003; Jain et al., 2006; Kramer et al., 2007; Pascual et al., 2008).

Data presented here have implications for our understanding of how mature differentiated cell types are maintained. Previous studies have indicated that the differentiated state is not irreversible because even mature specialized cells, including for example, olfactory neurons and mature T- and B-cells, can be reprogrammed into undifferentiated pluripotent cells by either somatic cell nuclear transfer or using the recently developed methodology for the generation of induced pluripotent stem cells (Takahashi and Yamanaka, 2006; Gurdon and Melton, 2008). Nevertheless, under normal nonmanipulated conditions *in vivo*, differentiated cells are remarkably stable, indicating the importance of mechanisms that maintain cells in their appropriate differentiated state. Gene targeting in non-neural cell types has revealed how transcription factors functioning in development can be important for the maintenance of terminally differentiated cell types, e.g., Pax5 in B-lymphocytes and Prox1 in lymphatic endothelial cells (Cobaleda et al., 2007; Johnson et al., 2008). In CNS, transcription factors identified for their key roles in early neuron development often continue to be expressed in the adult brain and may therefore guard against loss of phenotype or drift into alternative states (Smidt et al., 1997, 2000; Zetterström et al., 1997; Hendricks et al., 1999; Vult von Steyern et al., 1999; Albéri et al., 2004; Simon et al., 2004; Kang et al., 2007; Kittappa et al., 2007; Smidt and Burbach, 2007; Alavian et al.,

2008). However, remarkably little is known of how these factors function at late stages of development or in the adult. Although examples of adult mDA neuron loss has been reported in mice haploinsufficient for transcription factor genes such as *Engrailed* and *FoxA2*, it remains possible that defects originate during embryonic development (Albéri et al., 2004; Zhao et al., 2006; Kittappa et al., 2007; Sonnier et al., 2007). Importantly, FoxA2 and Engrailed are critical for the establishment of the floor plate and for early midbrain/hindbrain development, respectively, and they are directly and indirectly affecting many cell fates along the entire neuraxis. Thus, haploinsufficiency may cause embryonal deficiencies that do not become manifest until adult stages, a possibility that emphasizes the importance of temporally controlled conditional gene targeting to rigorously test how transcription factors function in terminally differentiated neurons.

We do not yet understand why Nurr1 is required in already differentiated mDA neurons. However, data presented here provide compelling evidence for the existence of "terminal selector genes" in mammalian CNS development. Such genes, defined from studies of *Caenorhabditis elegans* neuronal development, are continuously expressed throughout the life of neurons and are essential for both the establishment and maintenance of distinct neuronal phenotypes (Hobert, 2008). Thus, Nurr1, which probably regulates typical mDA neuron markers such as *TH*, *DAT*, *AADC*, and *VMAT2* (Sakurada et al., 1999; Sacchetti et al., 2001; Hermanson et al., 2003; Kim et al., 2003), is likely required for both early differentiation and maintenance by regulating genes that distinguish mDA neurons from other neuron types. Presumably, such regulation is critical throughout the life of mDA neurons and would depend on additional components, such as Pitx3, in a core transcription factor network (Jacobs et al., 2009).

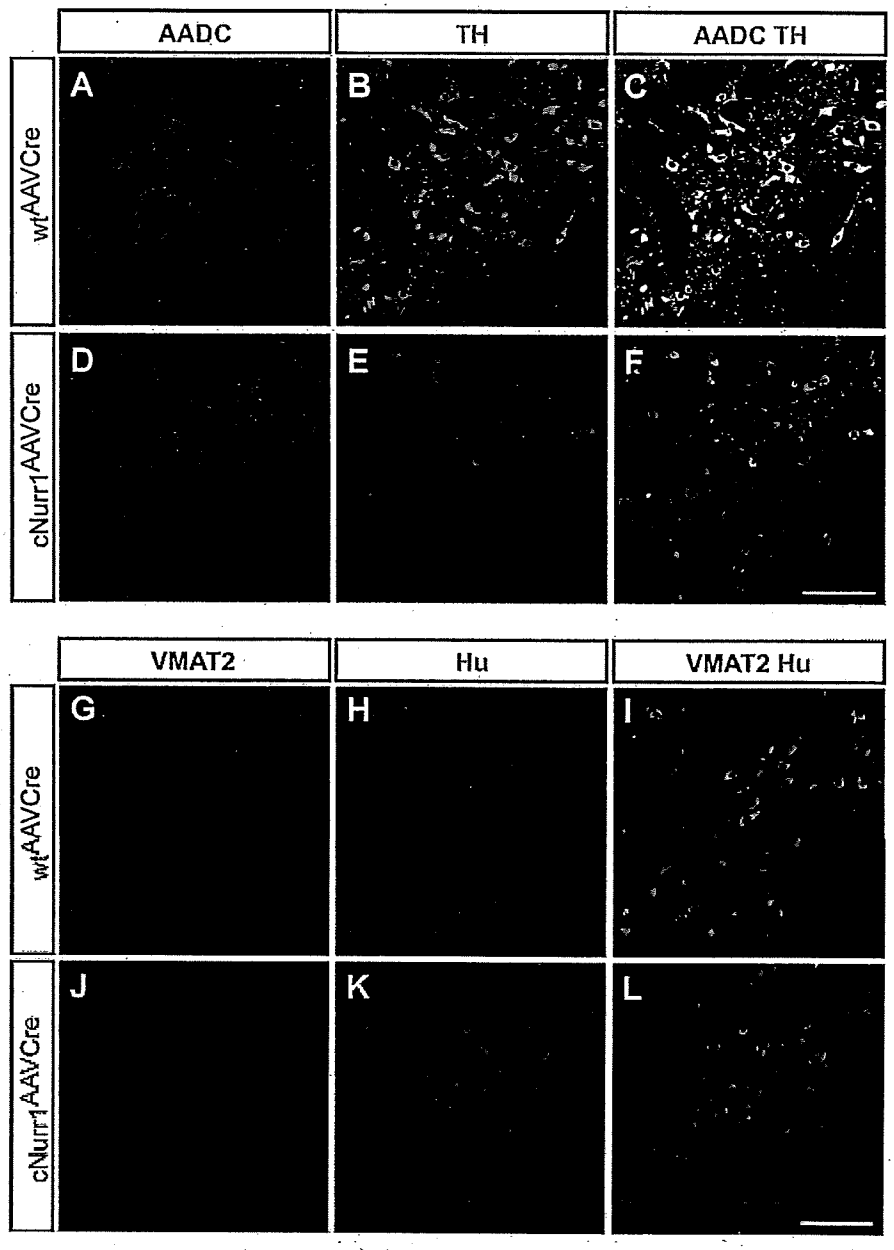

Figure 7. Decreased levels of VMAT2 but not AADC in $cNurr1^{AAVCre}$ mice. Confocal analysis of SNc in wt^{AAVCre} and $cNurr1^{AAVCre}$ mice at 4 months, as indicated. ***A–F***, Confocal images show staining of AADC (red; ***A***, ***D***), TH (green; ***B***, ***E***), and double staining of both markers (***C***, ***F***). Micrographs show that AADC expression appears expressed at normal levels in most cells with decreased levels of TH. ***G–L***, Confocal images show staining for VMAT2 (red; ***G***, ***J***), Hu (***H***, ***K***), and double staining of both markers (***I***, ***L***). Micrographs show that VMAT2 is severely decreased in $cNurr1^{AAVCre}$ mice, whereas Hu is maintained at normal levels in essentially all cells with decreased VMAT2. Scale bar, 200 μm.

How may dysregulated Nurr1 activity contribute to PD? Studies in PD patients have shown that, in early stages of the disease, SNc cell bodies are relatively spared compared with the loss of DA in the putamen (Fearnley and Lees, 1991) and that a significant fraction of the surviving, pigmented, DA somata in the SNc have much reduced expression of the TH enzyme (Hirsch et al., 1988; Chu et al., 2006). This suggests that, during early stages of disease, nigral DA neurons may survive in a dysfunctional state characterized by a downregulated neurotransmitter machinery. An interesting possibility supported by our data is that reduced expression of Nurr1 contributes to such symptoms. Indeed, Nurr1 is severely reduced in neurons with signs of pathology in PD brain tissue, and reduced Nurr1 expression in patients' peripheral blood lymphocytes indicates that diminished Nurr1 activity may be a systemic feature of disease (Chu et al., 2006; Le et al., 2008). Although such correlations do not determine whether reduced Nurr1 expression is a cause or a consequence of disease, progressive cell dysfunction in *Nurr1*-ablated mice provides a clear indication that diminished Nurr1 expression in PD should have deleterious consequences for patients. This view is supported by the identification of *Nurr1* gene variants that have been associated with rare cases of familial and sporadic PD (Xu et al., 2002; Le et al., 2003; Zheng et al., 2003; Jankovic et al., 2005; Grimes et al., 2006; Jacobsen et al., 2008). Although other studies have failed to identify such mutations and indicated that Nurr1

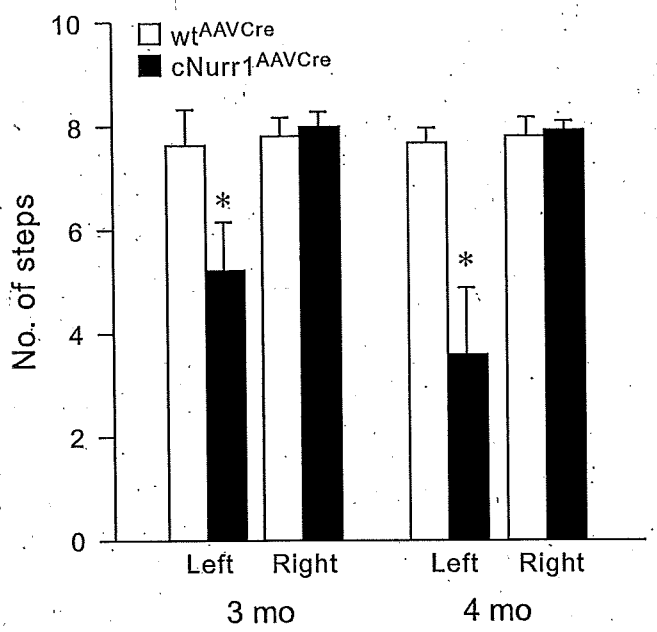

Figure 8. Forelimb akinesia in the stepping test. The performance of the left paw (contralateral to the vector injection) was significantly impaired in the fl/fl mice ($n = 16$) but not the wild-type mice ($n = 13$). Although the impairment was significant at both time points, 3 and 4 months after vector injection, their performance got significantly worse over time ($p < 0.01$, Student's paired t test): 15 of the 16 mice in the fl/fl group showed a decline in their stepping scores between the two tests, and at 4 months, 14 of the fl/fl mice had scores below 5 compared with 6 in the 3 month test. Scores give the means of steps recorded in the forehand and backhand direction for each paw (see Materials and Methods). *$p < 0.001$, Student's paired t test.

gene variants as a cause of PD must be very rare, the combined data from genetics, postmortem PD brain tissue analyses, and the ablation experiments reported here strongly imply that, if and when Nurr1 function is reduced, it will exaggerate PD progression and severity (Wellenbrock et al., 2003; Hering et al., 2004; Tan et al., 2004).

The results indicate that therapies that can restore Nurr1 activity in diseased but not yet degenerated mDA neurons could be of clinical relevance. We envision several strategies whereby Nurr1 activity could be increased. (1) Nurr1 belongs to the nuclear receptor family whose members are commonly regulated by small lipophilic ligands. The putative ligand binding domain of Nurr1 is unconventional and lacks a ligand-binding pocket, but Nurr1 forms heterodimers with retinoid X receptors (RXRs), and ligands activating these receptors can protect mDA neurons in culture (Wallen-Mackenzie et al., 2003; Wang et al., 2003). Thus, RXR may be a relevant target for ligand modulation of Nurr1-regulated processes. It will be important to investigate to what extent Nurr1–RXR heterodimers versus Nurr1 alone are important in pathways associated with the phenotype described in this paper. (2) Nurr1 activity is possible to modulate, for example, by the leukemia drug 6-mercaptopurine (Ordentlich et al., 2003). Although such drugs are pleiotropic and serious side effects are likely, other compounds with higher specificity may be possible to identify. (3) Therapies directed at increasing Nurr1 activity would be effective only as long as sufficient levels of Nurr1 are expressed in diseased neurons. Thus, treatments aimed at restoration of Nurr1 expression by gene delivery may prove advantageous. Using similar AAV vectors as administered in this study may be of particular interest because they have properties that are clinically favorable and are already used in clinical trials in PD patients (Check, 2007).

In conclusion, loss of Nurr1 at stages when characteristic features of mDA neurons are already apparent in the developing embryo or in fully differentiated adult neurons results in loss of mDA neuron-specific gene expression and neuron degeneration. These findings highlight the importance of developmental mechanisms also in the adult brain and clearly indicate that they may be critical for the understanding of cell maintenance and neurodegeneration. How Nurr1 and other transcription factors operate in adult neurons to control and prevent loss or drift in phenotype remains a challenge for future studies.

References

Alavian KN, Scholz C, Simon HH (2008) Transcriptional regulation of mesencephalic dopaminergic neurons: the full circle of life and death. Mov Disord 23:319–328.

Albéri L, Sgadò P, Simon HH (2004) Engrailed genes are cell-autonomously required to prevent apoptosis in mesencephalic dopaminergic neurons. Development 131:3229–3236.

Andersson E, Tryggvason U, Deng Q, Friling S, Alekseenko Z, Robert B, Perlmann T, Ericson J (2006) Identification of intrinsic determinants of midbrain dopamine neurons. Cell 124:393–405.

Breese GR, Knapp DJ, Criswell HE, Moy SS, Papadeas ST, Blake BL (2005) The neonate-6-hydroxydopamine-lesioned rat: a model for clinical neuroscience and neurobiological principles. Brain Res Brain Res Rev 48:57–73.

Castillo SO, Baffi JS, Palkovits M, Goldstein DS, Kopin IJ, Witta J, Magnuson MA, Nikodem VM (1998) Dopamine biosynthesis is selectively abolished in substantia nigra ventral tegmental area but not in hypothalamic neurons in mice with targeted disruption of the Nurr1 gene. Mol Cell Neurosci 11:36–46.

Check E (2007) Second chance. Nat Med 13:770–771.

Chu Y, Le W, Kompoliti K, Jankovic J, Mufson EJ, Kordower JH (2006) Nurr1 in Parkinson's disease and related disorders. J Comp Neurol 494:495–514.

Cobaleda C, Jochum W, Busslinger M (2007) Conversion of mature B cells into T cells by dedifferentiation to uncommitted progenitors. Nature 449:473–477.

Ekstrand MI, Terzioglu M, Galter D, Zhu S, Hofstetter C, Lindqvist E, Thams S, Bergstrand A, Hansson FS, Trifunovic A, Hoffer B, Cullheim S, Mohammed AH, Olson L, Larsson NG (2007) Progressive parkinsonism in mice with respiratory-chain-deficient dopamine neurons. Proc Natl Acad Sci U S A 104:1325–1330.

Fearnley JM, Lees AJ (1991) Ageing and Parkinson's disease: substantia nigra regional selectivity. Brain 114:2283–2301.

Grimes DA, Han F, Panisset M, Racacho L, Xiao F, Zou R, Westaff K, Bulman DE (2006) Translated mutation in the Nurr1 gene as a cause for Parkinson's disease. Mov Disord 21:906–909.

Gurdon JB, Melton DA (2008) Nuclear reprogramming in cells. Science 322:1811–1815.

Hendricks T, Francis N, Fyodorov D, Deneris ES (1999) The ETS domain factor Pet-1 is an early and precise marker of central serotonin neurons and interacts with a conserved element in serotonergic genes. J Neurosci 19:10348–10356.

Hering R, Petrovic S, Mietz EM, Holzmann C, Berg D, Bauer P, Woitalla D, Müller T, Berger K, Krüger R, Riess O (2004) Extended mutation analysis and association studies of Nurr1 (NR4A2) in Parkinson disease. Neurology 62:1231–1232.

Hermanson E, Joseph B, Castro D, Lindqvist E, Aarnisalo P, Wallén A, Benoit G, Hengerer B, Olson L, Perlmann T (2003) Nurr1 regulates dopamine synthesis and storage in MN9D dopamine cells. Exp Cell Res 288:324–334.

Hirsch E, Graybiel AM, Agid YA (1988) Melanized dopaminergic neurons are differentially susceptible to degeneration in Parkinson's disease. Nature 334:345–348.

Hobert O (2008) Regulatory logic of neuronal diversity: terminal selector genes and selector motifs. Proc Natl Acad Sci U S A 105:20067–20071.

Huot P, Parent A (2007) Dopaminergic neurons intrinsic to the striatum. J Neurochem 101:1441–1447.

Jacobs FM, van Erp S, van der Linden AJ, von Oerthel L, Burbach JP, Smidt MP (2009) Pitx3 potentiates Nurr1 in dopamine neuron terminal dif-

ferentiation through release of SMRT-mediated repression. Development 136:531–540.
Jacobsen KX, MacDonald H, Lemonde S, Daigle M, Grimes DA, Bulman DE, Albert PR (2008) A Nurr1 point mutant, implicated in Parkinson's disease, uncouples ERK1/2-dependent regulation of tyrosine hydroxylase transcription. Neurobiol Dis 29:117–122.
Jain S, Golden JP, Wozniak D, Pehek E, Johnson EM Jr, Milbrandt J (2006) RET is dispensable for maintenance of midbrain dopaminergic neurons in adult mice. J Neurosci 26:11230–11238.
Jankovic J, Chen S, Le WD (2005) The role of Nurr1 in the development of dopaminergic neurons and Parkinson's disease. Prog Neurobiol 77:128–138.
Johnson NC, Dillard ME, Baluk P, McDonald DM, Harvey NL, Frase SL, Oliver G (2008) Lymphatic endothelial cell identity is reversible and its maintenance requires Prox1 activity. Genes Dev 22:3282–3291.
Kang BJ, Chang DA, Mackay DD, West GH, Moreira TS, Takakura AC, Gwilt JM, Guyenet PG, Stornetta RL (2007) Central nervous system distribution of the transcription factor Phox2b in the adult rat. J Comp Neurol 503:627–641.
Kim KS, Kim CH, Hwang DY, Seo H, Chung S, Hong SJ, Lim JK, Anderson T, Isacson O (2003) Orphan nuclear receptor Nurr1 directly transactivates the promoter activity of the tyrosine hydroxylase gene in a cell-specific manner. J Neurochem 85:622–634.
Kirik D, Rosenblad C, Björklund A (1998) Characterization of behavioral and neurodegenerative changes following partial lesions of the nigrostriatal dopamine system induced by intrastriatal 6-hydroxydopamine in the rat. Exp Neurol 152:259–277.
Kittappa R, Chang WW, Awatramani RB, McKay RD (2007) The foxa2 gene controls the birth and spontaneous degeneration of dopamine neurons in old age. PLoS Biol 5:e325.
Kramer ER, Aron L, Ramakers GM, Seitz S, Zhuang X, Beyer K, Smidt MP, Klein R (2007) Absence of Ret signaling in mice causes progressive and late degeneration of the nigrostriatal system. PLoS Biol 5:e39.
Le W, Pan T, Huang M, Xu P, Xie W, Zhu W, Zhang X, Deng H, Jankovic J (2008) Decreased NURR1 gene expression in patients with Parkinson's disease. J Neurol Sci 273:29–33.
Le WD, Xu P, Jankovic J, Jiang H, Appel SH, Smith RG, Vassilatis DK (2003) Mutations in NR4A2 associated with familial Parkinson disease. Nat Genet 33:85–89.
Oo TF, Kholodilov N, Burke RE (2003) Regulation of natural cell death in dopaminergic neurons of the substantia nigra by striatal glial cell line-derived neurotrophic factor *in vivo*. J Neurosci 23:5141–5148.
Ordentlich P, Yan Y, Zhou S, Heyman RA (2003) Identification of the antineoplastic agent 6-mercaptopurine as an activator of the orphan nuclear hormone receptor Nurr1. J Biol Chem 278:24791–24799.
Pascual A, Hidalgo-Figueroa M, Piruat JI, Pintado CO, Gómez-Díaz R, López-Barneo J (2008) Absolute requirement of GDNF for adult catecholaminergic neuron survival. Nat Neurosci 11:755–761.
Perlmann T, Wallén-Mackenzie A (2004) Nurr1, an orphan nuclear receptor with essential functions in developing dopamine cells. Cell Tissue Res 318:45–52.
Sacchetti P, Brownschidle LA, Granneman JG, Bannon MJ (1999) Characterization of the 5′-flanking region of the human dopamine transporter gene. Brain Res Mol Brain Res 74:167–174.
Sacchetti P, Mitchell TR, Granneman JG, Bannon MJ (2001) Nurr1 enhances transcription of the human dopamine transporter gene through a novel mechanism. J Neurochem 76:1565–1572.
Sakurada K, Ohshima-Sakurada M, Palmer TD, Gage FH (1999) Nurr1, an orphan nuclear receptor, is a transcriptional activator of endogenous tyrosine hydroxylase in neural progenitor cells derived from the adult brain. Development 126:4017–4026.
Saucedo-Cardenas O, Quintana-Hau JD, Le WD, Smidt MP, Cox JJ, De Mayo F, Burbach JP, Conneely OM (1998) Nurr1 is essential for the induction of the dopaminergic phenotype and the survival of ventral mesencephalic late dopaminergic precursor neurons. Proc Natl Acad Sci U S A 95:4013–4018.
Schallert T, Norton D, Jones TA (1992) A clinically relevant unilateral rat model of Parkinsonian akinesia. J Neural Transpl Plast 3:332–333.
Simon HH, Thuret S, Alberi L (2004) Midbrain dopaminergic neurons: control of their cell fate by the engrailed transcription factors. Cell Tissue Res 318:53–61.
Smidt MP, Burbach JP (2007) How to make a mesodiencephalic dopaminergic neuron. Nat Rev Neurosci 8:21–32.
Smidt MP, van Schaick HS, Lanctôt C, Tremblay JJ, Cox JJ, van der Kleij AA, Wolterink G, Drouin J, Burbach JP (1997) A homeodomain gene Ptx3 has highly restricted brain expression in mesencephalic dopaminergic neurons. Proc Natl Acad Sci U S A 94:13305–13310.
Smidt MP, Asbreuk CH, Cox JJ, Chen H, Johnson RL, Burbach JP (2000) A second independent pathway for development of mesencephalic dopaminergic neurons requires Lmx1b. Nat Neurosci 3:337–341.
Smidt MP, Smits SM, Burbach JP (2004) Homeobox gene Pitx3 and its role in the development of dopamine neurons of the substantia nigra. Cell Tissue Res 318:35–43.
Snyder AM, Zigmond MJ, Lund RD (1986) Sprouting of serotoninergic afferents into striatum after dopamine-depleting lesions in infant rats: a retrograde transport and immunocytochemical study. J Comp Neurol 245:274–281.
Sonnier L, Le Pen G, Hartmann A, Bizot JC, Trovero F, Krebs MO, Prochiantz A (2007) Progressive loss of dopaminergic neurons in the ventral midbrain of adult mice heterozygote for Engrailed 1. J Neurosci 27:1063–1071.
Soriano P (1999) Generalized lacZ expression with the ROSA26 Cre reporter strain. Nat Genet 21:70–71.
Takahashi K, Yamanaka S (2006) Induction of pluripotent stem cells from mouse embryonic and adult fibroblast cultures by defined factors. Cell 126:663–676.
Tan EK, Chung H, Chandran VR, Tan C, Shen H, Yew K, Pavanni R, Puvan KA, Wong MC, Teoh ML, Yih Y, Zhao Y (2004) Nurr1 mutational screen in Parkinson's disease. Mov Disord 19:1503–1505.
Vult von Steyern F, Martinov V, Rabben I, Njå A, de Lapeyrière O, Lømo T (1999) The homeodomain transcription factors Islet 1 and HB9 are expressed in adult alpha and gamma motoneurons identified by selective retrograde tracing. Eur J Neurosci 11:2093–2102.
Wallen-Mackenzie A, Mata de Urquiza A, Petersson S, Rodriguez FJ, Friling S, Wagner J, Ordentlich P, Lengqvist J, Heyman RA, Arenas E, Perlmann T (2003) Nurr1-RXR heterodimers mediate RXR ligand-induced signaling in neuronal cells. Genes Dev 17:3036–3047.
Wang Z, Benoit G, Liu J, Prasad S, Aarnisalo P, Liu X, Xu H, Walker NP, Perlmann T (2003) Structure and function of Nurr1 identifies a class of ligand-independent nuclear receptors. Nature 423:555–560.
Wellenbrock C, Hedrich K, Schafer N, Kasten M, Jacobs H, Schwinger E, Hagenah J, Pramstaller PP, Vieregge P, Klein C (2003) NR4A2 mutations are rare among European patients with familial Parkinson's disease. Ann Neurol 54:415.
Xu PY, Liang R, Jankovic J, Hunter C, Zeng YX, Ashizawa T, Lai D, Le WD (2002) Association of homozygous 7048G7049 variant in the intron six of Nurr1 gene with Parkinson's disease. Neurology 58:881–884.
Zetterström RH, Williams R, Perlmann T, Olson L (1996) Cellular expression of the immediate early transcription factors Nurr1 and NGFI-B suggests a gene regulatory role in several brain regions including the nigrostriatal dopamine system. Brain Res Mol Brain Res 41:111–120.
Zetterström RH, Solomin L, Jansson L, Hoffer BJ, Olson L, Perlmann T (1997) Dopamine neuron agenesis in Nurr1-deficient mice. Science 276:248–250.
Zhao ZQ, Scott M, Chiechio S, Wang JS, Renner KJ, Gereau RW 4th, Johnson RL, Deneris ES, Chen ZF (2006) Lmx1b is required for maintenance of central serotonergic neurons and mice lacking central serotonergic system exhibit normal locomotor activity. J Neurosci 26:12781–12788.
Zheng K, Heydari B, Simon DK (2003) A common NURR1 polymorphism associated with Parkinson disease and diffuse Lewy body disease. Arch Neurol 60:722–725.

J Physiol 587.20 (2009) pp 4845–4862

The Journal of Physiology

Primary motor cortical metaplasticity induced by priming over the supplementary motor area

Masashi Hamada[1], Ritsuko Hanajima[1], Yasuo Terao[1], Shingo Okabe[1], Setsu Nakatani-Enomoto[2], Toshiaki Furubayashi[2], Hideyuki Matsumoto[1], Yuichiro Shirota[1], Shinya Ohminami[1] and Yoshikazu Ugawa[2]

[1]*Department of Neurology, Division of Neuroscience, Graduate School of Medicine, The University of Tokyo, Tokyo, Japan*
[2]*Department of Neurology, School of Medicine, Fukushima Medical University, Fukushima, Japan*

Motor cortical plasticity induced by repetitive transcranial magnetic stimulation (rTMS) sometimes depends on the prior history of neuronal activity. These effects of preceding stimulation on subsequent rTMS-induced plasticity have been suggested to share a similar mechanism to that of metaplasticity, a homeostatic regulation of synaptic plasticity. To explore metaplasticity in humans, many investigations have used designs in which both priming and conditioning are applied over the primary motor cortex (M1), but the effects of priming stimulation over other motor-related cortical areas have not been well documented. Since the supplementary motor area (SMA) has anatomical and functional cortico-cortical connections with M1, here we studied the homeostatic effects of priming stimulation over the SMA on subsequent rTMS-induced plasticity of M1. For priming and subsequent conditioning, we employed a new rTMS protocol, quadripulse stimulation (QPS), which produces a broad range of motor cortical plasticity depending on the interval of the pulses within a burst. The plastic changes induced by QPS at various intervals were altered by priming stimulation over the SMA, which did not change motor-evoked potential sizes on its own but specifically modulated the excitatory I-wave circuits. The data support the view that the homeostatic changes are mediated via mechanisms of metaplasticity and highlight an important interplay between M1 and SMA regarding homeostatic plasticity in humans.

(Received 21 July 2009; accepted after revision 31 August 2009; first published online 1 September 2009)
Corresponding author M. Hamada: Department of Neurology, Division of Neuroscience, Graduate School of Medicine, The University of Tokyo, 7-3-1, Hongo, Bunkyo-ku, Tokyo 113-8655, Japan. Email: mhamada-tky@umin.net

Abbreviations CS, conditioning stimulus; FDI, first dorsal interosseous muscle; ICF, intracortical facilitation; ISI, inter-stimulus intervals; ITT, inter-train interval; LICI, long-interval intracortical inhibition; LTD, long-term depression; LTP, long-term potentiation; M1, primary motor cortex; MEP, motor-evoked potential; PMd and PMv, dorsal and ventral premotor cortex; QPS, quadripulse stimulation; rTMS, repetitive transcranial magnetic stimulation; SICF, short-interval intracortical facilitation; SICI, short-interval intracortical inhibition; SMA, supplementary motor area; TA, right tibialis anterior muscle; TS, test stimulus.

Introduction

Repetitive transcranial magnetic stimulation (rTMS) is a promising method to induce plastic changes in humans (Hallett, 2007). In some cases, the rTMS-induced plasticity is *N*-methyl-D-aspartate (NMDA) dependent, supporting the idea that changes in synaptic efficacy, such as long-term potentiation (LTP) and long-term depression (LTD), are implicated in rTMS-induced plasticity (Stefan *et al.* 2002; Huang *et al.* 2007). Several human studies have also shown effects of a prior history of neuronal activity on subsequent rTMS-induced plasticity (e.g. Siebner *et al.* 2004; Hamada *et al.* 2008*a*). These findings have been compared with metaplasticity, homeostatic regulation of synaptic plasticity in which the capacity of synapses to exhibit plasticity depends on prior levels of neuronal activity (Abraham & Bear, 1996; Ziemann & Siebner, 2008). This form of plasticity regulation might relate directly to the Bienenstock–Cooper–Munro (BCM) theory, a prevailing model for homeostatic mechanisms of synaptic plasticity (Bienenstock *et al.* 1982; Abraham, 2008).

The protocol for studying metaplasticity in an experimental context is to apply a period of priming

DOI: 10.1113/jphysiol.2009.179101

stimulation (which on its own has little or no effect on synaptic plasticity) and then to test whether this changes the response to a second period of conditioning stimulation which produces LTP or LTD when given alone (Abraham, 2008). Many human studies have used designs in which both priming and conditioning are applied over the primary motor cortex (M1) (Iyer *et al.* 2003; Siebner *et al.* 2004; Lang *et al.* 2004; Müller *et al.* 2007; Hamada *et al.* 2008*a*). Others showed that metaplastic effects can be elicited by finger movements or voluntary muscle contraction, in place of priming stimulation, which might be associated with activity changes in cortical circuits within various motor-related areas (Ziemann *et al.* 2004; Gentner *et al.* 2008; Huang *et al.* 2008). More recently, Ragert *et al.* (2009) demonstrated the effects of priming stimulation over the right M1 on subsequent rTMS-induced plasticity of left M1 (Ragert *et al.* 2009). Of note is the fact that the effects of priming stimulation over motor-related areas other than ipsilateral or contralateral M1 have not been well documented, despite important anatomical and functional interplay between those areas and M1.

Among the motor-related areas, the lateral premotor cortex (PM) such as dorsal and ventral PM (PMd and PMv) has been extensively studied by means of TMS in humans to shed light on the interaction between M1 (see review by Reis *et al.* 2008). The supplementary motor area (SMA) also has dense cortico-cortical connections with M1 in animals (Dum & Strick, 1991; Luppino *et al.* 1993; Tokuno & Nambu, 2000) and plays a substantial role in higher motor control and learning (Tanji & Shima, 1994; Hikosaka *et al.* 1999; Nachev *et al.* 2008). However, as SMA is located in the interhemispheric fissure, it is a more difficult site to stimulate than the lateral PM (Reis *et al.* 2008). Thus, not much has been done in SMA as compared to PMd; two studies revealed that TMS over SMA can modulate the cortical excitability of M1 via cortico-cortical synaptic connections (Civardi *et al.* 2001; Matsunaga *et al.* 2005). In light of this accruing evidence, we aimed to explore the effects of preceding stimulation over SMA on subsequent rTMS-induced plasticity of the M1 in order to test the hypothesis that priming over the SMA modulates some cortical neurons within M1 via cortico-cortical connections, and that such prior history of neuronal activity alters subsequent rTMS-induced plasticity.

For priming and subsequent conditioning, we employed a new rTMS protocol, quadripulse stimulation (QPS) (Hamada *et al.* 2007, 2008*a*). QPS consists of repeated trains of four monophasic TMS pulses separated by inter-stimulus intervals (ISI) of 1.5–1250 ms, inducing bidirectional motor cortical plasticity in an ISI-dependent, non-linear form that are compatible with changes in synaptic plasticity. In addition, we showed that QPS interventions could interact in a metaplastic manner such that priming over M1 using QPS at short ISIs, which did not induce any plastic changes by itself, occluded subsequent LTP-like plasticity, whereas priming using QPS with long ISIs tended to do the reverse and increased the probability that facilitatory effects would be produced by a subsequent period of stimulation. The data support a BCM-like model of priming that shifts the crossover point at which the synaptic plasticity reverses from LTD to LTP. We proposed that such a broad range of after-effects produced by QPS facilitates detailed examinations of metaplasticity theories in humans (Hamada *et al.* 2008*a*). In the present study, we evaluated how LTD-like and LTP-like QPS-induced plasticity was altered by a preceding period of priming stimulation over SMA to understand metaplastic interplay between SMA and M1.

Methods

Subjects

Subjects were nine healthy volunteers (one woman, eight men; 27–45 years old, mean ± S.D., 34.5 ± 6.7 years) who gave their written informed consent to participate in the experiments. No subjects had neurological, psychiatric or other medical problems, or had any contraindication to TMS (Wassermann, 1998). All were right-handed according to the Oldfield handedness inventory (Oldfield, 1971). The protocol was approved by the Ethics Committee of the University of Tokyo and was carried out in accordance with the ethical standards of the *Declaration of Helsinki*. The procedures are in compliance with *The Journal of Physiology*'s guidelines for experimentation on humans (Drummond, 2009).

Recordings

Subjects were seated on a comfortable chair. The electromyogram (EMG) activity was recorded from the right first dorsal interosseous muscle (FDI) and the right tibialis anterior muscle (TA) using a belly-tendon arrangement. Responses were input to an amplifier (Biotop; GE Marquette Medical Systems, Japan) through filters set at 100 Hz and 3 kHz; they were then digitized and stored on a computer for later offline analyses (TMS bistim tester; Medical Try System, Japan).

Stimulation

Focal TMS was given using a hand-held figure-of-eight coil (9 cm external diameter at each wing; The Magstim Co. Ltd, Whitland, Dyfed, UK). Single monophasic TMS pulses were delivered by a magnetic stimulator (Magstim 200; The Magstim Co. Ltd). Quadripulse stimuli were delivered by four magnetic stimulators (Magstim 200^2; The Magstim Co. Ltd) connected with a specially designed

combining module (The Magstim Co. Ltd). This device combines the outputs from four stimulators to allow a train of four monophasic magnetic pulses to be delivered through a single coil.

The optimal site for eliciting MEPs from the right FDI muscle (i.e. hot spot for FDI) was determined before each experiment and considered to be the primary motor cortex for FDI muscle ($M1_{FDI}$). A figure-of-eight coil was placed tangentially over the scalp with the handle pointing backwards at about 45 deg laterally. We stimulated several positions in 1 cm increments in the anterio-posterior and medio-lateral direction from each other using the same intensity and determined $M1_{FDI}$ as the site at which the largest responses were elicited. This position was marked with a blue pen on the scalp for repositioning the coil. The resting motor threshold for FDI (RMT_{FDI}) was defined as the lowest intensity that evoked a response of at least 50 μV in the relaxed FDI in at least 5 of 10 consecutive trials (Rossini *et al.* 1994). The active motor threshold for FDI (AMT_{FDI}) was defined as the lowest intensity that evoked a small response (>100 μV) when the subjects maintained a slight contraction of the right FDI (~10% of the maximum voluntary contraction), as observed using an oscilloscope monitor, in more than 5 of 10 consecutive trials. The stimulus intensity was changed in steps of 1% of the maximum stimulator output (MSO).

SMA stimulation was given with a coil centred at a point 3 cm anterior to the optimal site for eliciting MEPs in the right TA muscle (i.e. hot spot for TA) according to previous studies (Hikosaka *et al.* 1996; Lee *et al.* 1999; Terao *et al.* 2001; Matsunaga *et al.* 2005). The hot spot for TA was determined by moving the coil in 1 cm steps along the sagittal mid-line through the vertex (Cz) with the handle pointing to the right until we detected the position which evoked the largest MEP. This was considered to be the primary motor cortex for the TA muscle ($M1_{TA}$). We then used this position to determine the AMT for TA (AMT_{TA}). On average, the site of SMA stimulation (i.e. the point 3 cm anterior to $M1_{TA}$) was 2–3 cm anterior to Cz, in line with data from previous studies (Hikosaka *et al.* 1996; Lee *et al.* 1999; Matsunaga *et al.* 2005).

Measurement of motor cortical excitability

Motor cortical excitability was assessed by measuring the peak-to-peak amplitude of MEPs from the relaxed right FDI muscle elicited by single pulse TMS over the left $M1_{FDI}$ for all experiments. The stimulus intensity was adjusted to produce MEPs of about 0.5 mV in the right FDI muscle. During the experiments, EMG activity of the FDI was monitored with an oscilloscope monitor. Trials contaminated with voluntary EMG activities were discarded from analyses.

Quadripulse stimulation

The QPS protocol consisted of trains of TMS pulses with an inter-train interval (ITI) of 5 s (i.e. 0.2 Hz). Each train consisted of four magnetic pulses separated by inter-stimulus intervals (ISI) of 1.5, 5, 10, 30, 50 or 100 ms. These conditioning types were designated as QPS-1.5 ms to QPS-100 ms, respectively.

Experiment 1: Effects of SMA priming on subsequent QPS-induced plasticity

Six of nine subjects were enrolled. The experimental sessions were separated by 1 week or longer in the same subject. The order of the experiments was randomized and balanced among subjects.

Experiment 1a: QPS-induced plasticity without priming over SMA (Fig. 1). To investigate QPS-induced plasticity without any priming, conditioning stimulation was applied over the left $M1_{FDI}$ using QPS at various ISIs (QPS-1.5 ms, QPS-5 ms, QPS-10 ms, QPS-30 ms, QPS-50 ms and QPS-100ms) for 30 min (Fig. 1). The stimulus intensity of each pulse for QPS conditioning was set at 90% AMT_{FDI} (Hamada *et al.* 2008*a*). During the conditioning, no MEPs were observed.

Before QPS, 20 MEPs were obtained every 14.5–15.5 s using single-pulse TMS at a fixed intensity. The stimulus intensity was adjusted to produce MEPs of about 0.5 mV in the right FDI muscle at baseline (B1 in Fig. 1); the intensity was kept constant throughout the same experiment. After QPS conditioning, MEPs were measured every 5 min for 30 min. At each time point of the measurements, MEPs were collected in the same manner as baseline measurements.

Experiment 1b: QPS-induced plasticity with QPS-5 ms priming over SMA (Fig. 1). Priming stimulation was applied over SMA using QPS-5 ms for 10 min (i.e. four pulses at an ISI of 5 ms with an ITI of 5 s for 10 min). Importantly, priming over SMA using QPS-5 ms for 10 min induces no substantial effects on MEP sizes (see Results). The aim of the experiment was to test whether this priming stimulation would have effects on subsequent QPS-induced plasticity according to previous animal studies, which showed that prior induction of LTP is not prerequisite for metaplasticity (Abraham & Tate, 1997; Abraham, 2008). The stimulus intensity of each pulse for priming was set at 90% AMT_{TA}, which was identical to about 130% AMT_{FDI} (i.e. 90% RMT_{FDI}) (Table 1). The stimulus intensity used for priming over SMA was calculated relative to AMT_{TA} in order to secure effective stimulation of SMA, given that its depth is almost the same as that of the M1 for foot muscles in the

interhemispheric fissure. Additionally, 130% AMT of hand muscle over SMA has been considered not to spread to the PMd or M1 (Matsunaga *et al.* 2005).

Subsequent conditioning was applied over the left $M1_{FDI}$ using QPS at various ISIs (QPS-1.5 ms, QPS-5 ms, QPS-10 ms, QPS-30 ms, QPS-50 ms and QPS-100ms) for 30 min (i.e. 360 trains, 1440 pulses in total) (Fig. 1). The stimulus intensity of each pulse for this subsequent conditioning was set at 90% AMT_{FDI}.

Before the priming stimulation (B0 in Fig. 1), 20 MEPs were collected every 14.5–15.5 s using single-pulse TMS at a fixed intensity, which was adjusted to elicit MEPs of about 0.5 mV in the right FDI muscle at B0 and kept constant throughout the experiment. After priming over SMA, 20 MEPs were again obtained in the same manner as measurements at B0 (B1 in Fig. 1). Following this measurement at B1 (i.e. immediately after priming), QPS conditioning of various types over the left $M1_{FDI}$ was performed. After each QPS, MEPs were measured every 5 min for 30 min (Fig. 1).

Experiment 1c: QPS-induced plasticity with QPS-50 ms priming over SMA (Fig. 1). QPS-50 ms for 10 min (i.e. four pulses at an ISI of 50 ms with an ITI of 5 s for 10 min) was selected as another priming stimulation over SMA to reveal the opposite priming effects to QPS-5 ms priming. The stimulus intensity for each pulse was set at 90% AMT_{TA}. Subsequent conditioning types after QPS-50 ms priming over SMA were QPS-5 ms, QPS-10 ms, QPS-30 ms and QPS-100 ms over the left $M1_{FDI}$ for 30 min. We have previously shown that QPS-50 ms priming over M1 produced substantial changes in subsequent QPS-induced plasticity at ISIs of

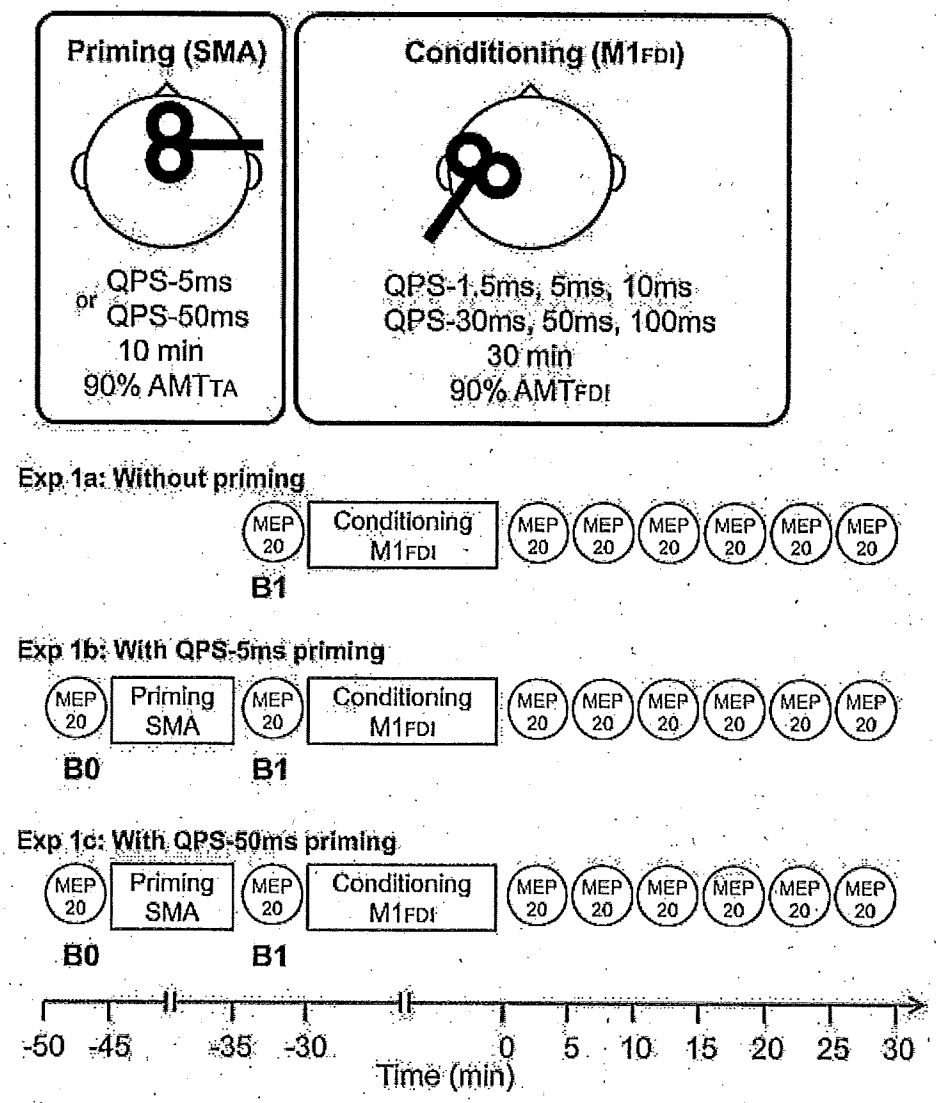

Figure 1. Timelines of experiments
(See Methods.)

Table 1. Physiological parameters (mean ± s.d.)

	RMT_{FDI}	AMT_{FDI}	AMT_{TA}	Stimulus intensify for SMA priming (relative to RMT_{FDI})	MEP size (mV), right FDI	
Experiment 1a: Without priming		Baseline (B1)				B1
QPS-1.5 ms	57.1 ± 9.8%	40.8 ± 6.9%	–	–	–	0.46 ± 0.11
QPS-5 ms	58.5 ± 9.5%	43.6 ± 5.1%	–	–	–	0.51 ± 0.13
QPS-10 ms	61.8 ± 10.9%	41.0 ± 6.6%	–	–	–	0.48 ± 0.16
QPS-30 ms	61.2 ± 11.6%	40.6 ± 5.8%	–	–	–	0.49 ± 0.09
QPS-50 ms	60.5 ± 14.1%	42.6 ± 5.4%	–	–	–	0.51 ± 0.18
QPS-100 ms	60.1 ± 12.1%	40.8 ± 5.8%	–	–	–	0.55 ± 0.06
Experiment 1b: With QPS-5 ms priming over SMA		Baseline (B1)		Mean ± s.d. (range)	B0	B1
QPS-1.5 ms	61.8 ± 9.2%	40.3 ± 1.9%	60.2 ± 8.0%	89 ± 8% (76–98%)	0.51 ± 0.09	0.49 ± 0.14
QPS-5 ms	59.8 ± 6.9%	42.8 ± 5.0%	60.8 ± 8.5%	92 ± 5% (85–97%)	0.43 ± 0.11	0.47 ± 0.28
QPS-10 ms	60.0 ± 9.7%	42.0 ± 4.9%	61.1 ± 10.0%	93 ± 4% (87–99%)	0.48 ± 0.18	0.54 ± 0.14
QPS-30 ms	58.3 ± 8.5%	41.7 ± 5.4%	60.8 ± 10.0%	95 ± 6% (86–100%)	0.51 ± 0.14	0.55 ± 0.18
QPS-50 ms	61.8 ± 7.6%	41.0 ± 5.1%	63.6 ± 8.1%	93 ± 5% (85–98%)	0.53 ± 0.21	0.53 ± 0.20
QPS-100 ms	60.8 ± 8.7%	40.3 ± 5.0%	61.5 ± 7.6%	92 ± 4% (86–96%)	0.53 ± 0.18	0.59 ± 0.21
Experiment 1c: With QPS-50 ms priming over SMA		Baseline (B1)			B0	B1
QPS-5 ms	61.6 ± 9.4%	41.6 ± 5.3%	62.6 ± 9.3%	94 ± 3% (91–98%)	0.50 ± 0.09	0.52 ± 0.08
QPS-10 ms	60.6 ± 9.1%	43.8 ± 5.9%	63.5 ± 9.6%	95 ± 2% (92–98%)	0.57 ± 0.11	0.53 ± 0.21
QPS-30 ms	58.1 ± 9.9%	42.1 ± 4.8%	62.2 ± 11.4%	95 ± 5% (88–100%)	0.53 ± 0.09	0.48 ± 0.04
QPS-100 ms	60.5 ± 10.1%	42.0 ± 6.4%	65.2 ± 11.7%	97 ± 3% (93–100%)	0.52 ± 0.12	0.49 ± 0.16
Experiment 2		Baseline (B0)			B0	B1
Sham with priming	61.8 ± 13.7%	40.8 ± 7.8%	61.5 ± 7.2%	93 ± 4% (88–100%)	0.46 ± 0.06	0.51 ± 0.14
QPS-10 ms with sham priming	58.3 ± 7.4%	40.5 ± 7.4%	–	–	0.47 ± 0.12	0.48 ± 0.18
Experiment 3		Baseline			Baseline	Post 1	Post 2
QPS-5 ms priming	60.6 ± 11.0%	42.0 ± 8.2%	66.0 ± 7.7%	95 ± 4% (88–100%)	0.52 ± 0.24	0.54 ± 0.27	0.49 ± 0.26
QPS-50 ms priming	59.7 ± 10.1%	41.5 ± 9.8%	66.4 ± 8.3%	95 ± 5% (88–100%)	0.48 ± 0.14	0.53 ± 0.19	0.55 ± 0.11
Experiment 4					ISI 3 ms	ISI 6 ms	
	57.9 ± 9.6%	43.3 ± 7.8%	62.6 ± 9.4%	–	0.59 ± 0.23	0.58 ± 0.27	

10, 30 and 100 ms (Hamada *et al.* 2008*a*). Since it would be of value to compare those results and SMA priming effects in the present study to understand the difference in priming stimulation site (i.e. M1 *versus* SMA), we selected the four ISIs used in the previous paper for Experiment 1c. The stimulus intensity of each pulse of QPS conditioning was set at 90% AMT_{FDI}. MEP measurements were exactly the same as those of Experiment 1b.

Experiment 2: Control experiments

In the first control experiment (Fig. 6*A*), priming stimulation using QPS-5 ms over SMA for 10 min was followed by sham conditioning stimulation (i.e. sham with priming) to examine whether the priming alone affects motor cortical excitability. In the second control experiment (Fig. 6*B*), sham priming stimulation was followed by QPS-10 ms over M1 to confirm that sham priming did not affect the QPS-induced plastic changes (QPS-10 ms with sham priming). QPS-10 ms was chosen as conditioning because this protocol induced mild facilitatory after-effects (see Results) which we thought might make it more susceptible to any bidirectional effects of sham priming.

The sham stimulation procedure used for these control experiments was identical to those described in our previous reports (Okabe *et al.* 2003; Hamada *et al.* 2008*b*). In

brief, four electric pulses (each electric pulse was of 0.2 ms duration with intensity of twice the sensory threshold) were given to the scalp at 0.2 Hz at an ISI of 10 ms for sham conditioning (first control experiment) and at 5 ms for sham priming (second control experiment) with a conventional electric peripheral nerve stimulator to mimic the skin sensation of TMS. Electric pulses were applied through the electrodes placed over the left $M1_{FDI}$ or SMA and the vertex. A coil, which was disconnected from the stimulator, was placed over the left $M1_{FDI}$ or SMA to mimic real TMS. Another coil, which was connected to a combining module with four stimulators, was held off the scalp but placed near the subject. This coil was discharged simultaneously with the scalp electrical stimulation to produce a similar sound to that associated with real QPS.

Experiment 3: Effects of priming over SMA on intracortical circuits of M1

Nine subjects participated in this experiment. To explore the effects of SMA priming alone on either excitatory or inhibitory circuits of M1, short-interval intracortical inhibition (SICI), intracortical facilitation (ICF) (Kujirai *et al.* 1993), short-interval intracortical facilitation (SICF) (Tokimura *et al.* 1996; Ziemann *et al.* 1998; Hanajima *et al.* 2002), and long-interval intracortical inhibition (LICI) (Valls-Sole *et al.* 1992; Wassermann *et al.* 1996) were measured using the paired-pulse technique before and after QPS-5 ms or QPS-50 ms priming over SMA (i.e. four pulses at an ISI of 5 ms or 50 ms with an ITI of 5 s for 10 min; the stimulus intensity of each pulse, 90% AMT_{TA}).

SICI was examined at an ISI of 3 ms using a conditioning stimulus (CS) intensity of 80% AMT_{FDI}. ICF was measured at an ISI of 10 ms with a CS intensity of 90% AMT_{FDI}. SICF was measured at an ISI of 1.5 ms. The intensity of the second stimulus (S2) was set at 10% below AMT_{FDI}. LICI was measured at an ISI of 100 ms with a CS intensity of 110% RMT_{FDI}. The intensity of the test stimulus (TS) (i.e. the first stimulus (S1) for SICF) was adjusted to elicit MEPs of 0.4–0.5 mV from relaxed FDI at baseline. Twelve trials were recorded for each condition and randomly intermixed with 18 trials of TS alone with an ITI of 5.5–6.5 s (about 6 min in total). The SICI, ICF, SICF and LICI were all studied simultaneously in one session using the four magnetic stimulators (i.e. three stimulators produced the different CS and the other one gave TS). Measurements of these values were performed in blocks immediately before (baseline) and just after QPS-5 ms priming (post 1) as well as 20 to 26 min (post 2). Conditioning intensities and test intensity were not changed after the priming because the test MEP sizes were not altered by SMA priming (see Results and Table 1).

Experiment 4: Supplementary experiments

The aim of these experiments was to test whether the conditioning stimulus over SMA spreads to M1 or PMd (Experiment 4a), or whether it exerts a direct effect on the spinal motor neurons (Experiment 4b). Eight subjects participated in this series of experiments.

Experiment 4a: Effects of a conditioning stimulus over SMA on MEP. We investigated whether the stimulus over SMA spreads to other cortical areas using a paired-pulse technique. The test response in the right relaxed FDI elicited by single pulse TMS over the left $M1_{FDI}$ was conditioned by single pulse TMS over SMA at an ISI of 3 ms or 6 ms. The intensity of the TS was adjusted to elicit MEPs of about 0.5 mV in the relaxed FDI when given alone. The stimulus intensities for conditioning over SMA were set at 70, 90 and 110% AMT_{TA}. At each ISI (i.e. 3 or 6 ms), 12 trials were recorded for each condition (70, 90 and 110% AMT_{TA}) and randomly intermixed with 18 trials of TS alone with an ITI of 5.5–6.5 s in a single block. Thus, two blocks of measurements at each ISI were performed. The order of blocks was randomized. As the inhibitory interneurons of the $M1_{FDI}$ might have a lower threshold than the intrinsic I-wave circuits (Reis *et al.* 2008), we argued that, if the current over SMA spread to the $M1_{FDI}$, then some inhibitory effects on the test response would be observed at an ISI of 3 ms in a conditioning intensity-dependent manner. Indeed, it is known that conditioning over the PMd at an ISI of 6 ms has either inhibitory or facilitatory effects on MEP sizes depending on the conditioning intensity (Civardi *et al.* 2001). Thus, we argued that, if the current over SMA spread to PMd, then some inhibitory or facilitatory effects on the test response would be observed in an intensity-dependent manner.

Experiment 4b: Effects of a stimulus over SMA on MEP in active condition. To test whether the current over SMA spreads to the $M1_{FDI}$ directly and whether direct stimulation of SMA activates some neurons in SMA projecting to the spinal motor neurons directly (Dum & Strick, 1991, 1996), single pulse TMS was applied over SMA during contraction of the right FDI muscle (20% maximum voluntary contraction). If the current over SMA spread to $M1_{FDI}$ directly or if the current stimulated some SMA neurons enough to produce any descending volley, then small MEPs would be elicited during voluntary contraction in an intensity-dependent manner. Ten stimuli were applied every 5 s at an intensity of 100% AMT_{TA}. The stimulus intensity was then increased by 10% of AMT_{TA} and another 10 stimuli were applied. This process was repeated until the intensity reached 190% AMT_{TA} or 100% MSO.

Data analyses

Experiment 1a. The after-effects of different conditioning types were analysed with absolute MEP amplitudes using two-way repeated-measures analysis of variance (ANOVA) (within-subject factors, CONDITION (QPS-1.5 ms, QPS-5 ms, ···, QPS-100ms), and TIME (B1 and following six time points)). If the factors CONDITION and TIME showed a significant interaction, *post hoc* paired t tests (two-tailed) with Bonferroni's corrections for multiple comparisons were used for further analyses. The Greenhouse–Geisser correction was used if necessary to correct for non-sphericity; P values less than 0.05 were considered significant.

Experiment 1b and 1c. Absolute values of MEPs at B0 and B1 (Fig. 1) were compared using paired t tests in each experiment. To evaluate the priming effects on subsequent QPS-induced plasticity, the absolute amplitudes of MEPs collected in Experiment 1a (i.e. without priming) and Experiment 1b (i.e. with QPS-5 ms priming over the SMA) or Experiment 1c (i.e. with QPS-50 ms priming over the SMA) were entered in three-way repeated-measures ANOVA with PRIMING (with and without priming), CONDITION ((QPS-1.5 ms, QPS-5 ms, ···, and QPS-100ms) for Experiment 1b, and (QPS-5 ms, QPS-10 ms, QPS-30 ms and QPS-100ms) for Experiment 1c), and TIME (B1, and following six time points) as within-subject factors to match the measurement time points relative to QPS conditioning among experiments. Additionally, it might be valid to evaluate the effect of priming stimulation on subsequent QPS-induced plasticity using these values because the absolute amplitudes obtained at B0 and B1 were not significantly different (see Results). If the factors PRIMING, CONDITION and TIME showed a significant interaction, *post hoc* paired t tests (two-tailed) with Bonferroni's corrections for multiple comparisons were used.

Experiment 2. The time course of after-effects for the first control experiment (i.e. sham conditioning with real priming) on absolute MEP sizes was analysed using one-way repeated measures ANOVA (within-subject factor, TIME (B1 and following six points)). For the second control experiment, the after-effects of QPS-10 ms with sham priming were compared with those of QPS-10 ms without priming using two-way repeated-measures ANOVA (within-subject factors, CONDITION (QPS-10 ms with sham priming, QPS-10 ms without priming) and TIME (B1 and following six points)).

Experiment 3. The ratio of the mean amplitude of the conditioned response to that of the control response was calculated for each condition in each subject. These individual mean ratios were then averaged to give a grand mean ratio. The time course of after-effects was analysed using three-way repeated measures ANOVA (within-subject factors, PRIMING (QPS-5 ms and QPS-50ms), BISTIM (SICI, ICF, SICF and LICI) and TIME (baseline, post 1 and post 2)). If the factors PRIMING, BISTIM and TIME showed a significant interaction, Dunnett's *post hoc* test in each condition was used for further analyses.

Experiment 4a. The ratio of the mean amplitude of the conditioned response to that of the control response was calculated for each condition in each subject. These individual mean ratios were then averaged to give a grand mean ratio. The ratios were entered in one-way repeated measures ANOVA (within-subject factor, INTENSITY of conditioning stimulation). Paired t tests (two-tailed) were used for further analyses.

Data were analysed with the commercialized software (SPSS version 17.0 for Windows; SPSS Inc.). All figures depict the group data.

Results

None of the subjects reported any adverse effects during or after any of the experiments. Baseline physiological data did not differ significantly among different experiments (Table 1). The stimulus intensities for SMA priming were all below RMT_{FDI} (Table 1).

Experiment 1: Effects of SMA priming on subsequent QPS-induced plasticity

Experiment 1a: QPS-induced plasticity without priming over SMA. In line with our previous report (Hamada *et al.* 2008*a*), QPS at short ISIs (QPS-1.5 ms, QPS-5 ms and QPS-10ms) produced an increase in the MEP amplitude, whereas QPS at long ISIs (QPS-30 ms, QPS-50 ms and QPS-100ms) suppressed MEPs (Fig. 2*A*). Two-way repeated measures ANOVA revealed a significant CONDITION (QPS-1.5 ms, QPS-5 ms, ···, and QPS-100ms) × TIME interaction ($F_{(2.941,14.705)} = 4.384$, $P < 0.001$). Figure 2*B* presents the MEP amplitude normalized to the baseline MEP at 30 min after QPS as a function of the reciprocal of the ISI used in each QPS burst. There was a non-linear relation between MEP excitability changes and ISI indicating the presence of threshold for inducing LTP-like plasticity. *Post hoc* analysis revealed that QPS-1.5 ms, QPS-5 ms and QPS-50ms were significantly different from QPS-30 ms.

Experiment1b: QPS-induced plasticity with QPS-5 ms priming over SMA. Figure 3 shows the time courses

of MEP amplitude following QPS at various ISIs with and without QPS-5 ms priming over SMA. No difference was found in MEP amplitudes at B0 and B1 in any conditions (paired t test, $P > 0.5$). Although SMA priming with QPS-5 ms did not occlude MEP facilitation by QPS-1.5 ms, it produced lasting MEP suppression after QPS-5 ms, QPS-10 ms and QPS-30 ms (Fig. 3*B–D*). By contrast, MEP suppression induced by QPS-50 ms and QPS-100 ms was not enhanced, but its duration was shortened by SMA priming (Fig. 3*E* and *F*). Three-way repeated measures ANOVA revealed a significant PRIMING × CONDITION × TIME interaction ($F_{(3.464,17.319)} = 3.826$, $P = 0.025$). *Post hoc* paired t tests revealed a significant effect of SMA priming on the after-effects of QPS-5 ms, QPS-10 ms, QPS-30 ms, QPS-50 ms and QPS-100 ms (Fig. 3*A–F*).

Experiment 1c: QPS-induced plasticity with QPS-50 ms priming over SMA. Figure 4 shows the change in MEP amplitude following QPS at various ISIs with and without QPS-50 ms priming over SMA. No difference in MEP amplitude was found at B0 and B1 in any conditions (paired t test, $P > 0.5$). QPS-50 ms priming over SMA did not enhance MEP facilitation by QPS-5 ms. It produced slight enhancement of MEP facilitation by QPS-10 ms (Fig. 4*A* and *B*). In contrast, transient MEP suppression induced by QPS-30 ms turned to facilitation after SMA priming, but there was no change in the after-effects of QPS-100 ms (Fig. 4*C* and *D*). Three-way repeated measures ANOVA revealed a significant PRIMING × CONDITION interaction ($F_{(2.593,9.948)} = 5.612$, $P = 0.023$), but revealed no significant PRIMING × CONDITION × TIME interaction ($F_{(3.363,16.810)} = 3.079$, $P = 0.051$). The results reveal that priming stimulation affected subsequent QPS-induced plasticity, irrespective of the time after QPS conditioning. *Post hoc* paired t tests revealed a significant effect of SMA priming with QPS-50 ms on the after-effects of QPS-5 ms and QPS-30 ms (Fig. 4*A* and *C*).

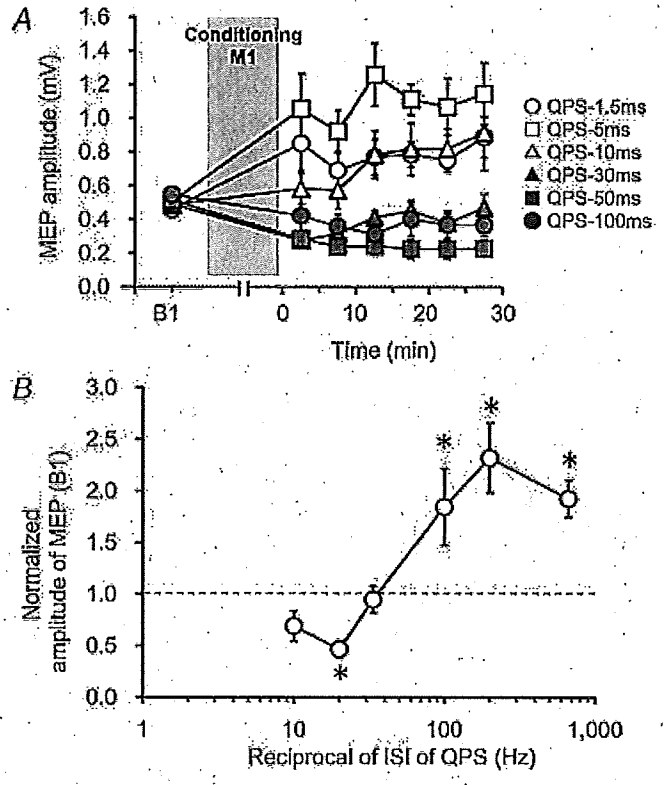

Figure 2. QPS-induced plasticity without priming over SMA
A, time courses of MEP amplitude following QPS at various ISIs without priming (mean ± S.E.M.). *B*, stimulus–response function of QPS-induced plasticity. Normalized amplitudes of MEP measured at 30 min after QPS as a function of the reciprocal of ISI of QPS: mean (± S.E.M.) of baseline. Note that the x-axis is logarithmic. Asterisks denote significant difference from QPS-30 ms (*$P < 0.05$).

Stimulus–response function with priming over SMA. The normalized MEP amplitudes at 30 min post conditioning are plotted as a function of the reciprocal of the ISI used in each QPS with and without priming over SMA (Fig. 5). The crossover point from MEP suppression to facilitation appears to shift in either direction along the x-axis according to which priming stimulation was employed. *Post hoc* analysis revealed that QPS-5 ms priming over SMA significantly reduced MEP sizes after QPS-5 ms, QPS-10 ms and QPS-30 ms, but occluded MEP suppression by QPS-50 ms. QPS-50 ms priming over SMA inhibited MEP sizes after QPS-5 ms, whereas it facilitated MEP sizes after QPS-30 ms (Fig. 5).

Experiment 2: Control experiments

First, the after-effects of sham conditioning with real priming were monitored to examine whether priming alone (i.e. QPS-5 ms over SMA for 10 min) affects motor cortical excitability. Figure 6*A* shows the time course of the MEP amplitude following sham conditioning with real priming. No difference was found in MEP amplitudes at B0 and B1 (paired t test, $P > 0.5$). Sham conditioning with real priming did not change the MEP amplitude for at least 30 min after conditioning (one-way repeated measures ANOVA: effect of TIME, $F_{(6,30)} = 0.410$, $P = 0.866$). Second, the after-effect of real conditioning (QPS-10ms) with sham priming was compared to that of real conditioning without priming to confirm that sham priming did not affect motor cortical plasticity induced by real conditioning. Figure 6*B* shows the absolute amplitude of MEPs following real conditioning (QPS-10ms) without priming and with sham priming. No difference was found between MEPs at B0 and B1 (paired t test, $P > 0.5$). Furthermore, MEP amplitudes following QPS-10 ms with sham priming

were not different from those without priming (two-way repeated measures ANOVA: effect of CONDITION (QPS-10 ms with sham priming, QPS-10 ms without priming), $F_{(1,5)} = 0.095$, $P = 0.770$; CONDITION × TIME interaction, $F_{(6,30)} = 0.410$, $P = 0.866$).

Experiment 3: Effects of priming over SMA on intracortical circuits of M1

Figure 7 shows the effects of priming over SMA on SICI, ICF, SICF and LICI. Three-way repeated measures ANOVA revealed significant PRIMING × BISTIM × TIME interaction ($F_{(6,48)} = 2.498$, $P = 0.035$). *Post hoc* tests revealed that only SICF was modulated after SMA priming; the effects on SICF were transient, being significant only at post 1 (Fig. 7*A* and *B*).

Experiment 4: Supplementary experiments

Experiment 4a: Effects of a conditioning stimulus over the SMA on MEP. Using the paired-pulse technique at an ISI of 3 ms, we investigated whether the stimulus over SMA spreads to $M1_{FDI}$. Figure 8*A* shows the changes of conditioned MEP relative to the unconditioned MEP in each block using three different conditioning intensities. One-way repeated measures ANOVA revealed a significant main effect of INTENSITY ($F_{(2,14)} = 3.904$, $P = 0.045$). *Post hoc* paired *t* tests revealed that the test MEPs were significantly inhibited by conditioning stimulus at 110% AMT_{TA} ($t = 2.39$, $P = 0.048$), whereas no significant inhibition was found at 70% or 90% AMT_{TA}.

Figure 8*B* shows the changes of conditioned MEP relative to the unconditioned MEP using the paired-pulse technique at an ISI of 6 ms. No significant effect of conditioning intensity over SMA at an ISI of 6 ms was found (one-way repeated measures ANOVA: effect of INTENSITY, $F_{(2,14)} = 0.679$, $P = 0.523$).

Experiment 4b: effects of a stimulus over the SMA on MEP in active condition. To test whether the current induced by TMS over the SMA directly spreads to the $M1_{FDI}$, single pulse TMS was applied over SMA during contraction of the right FDI muscle (20% maximum). Although the stimulus intensity reached 190% AMT_{TA} or 100% MSO, no MEPs were recorded in any condition.

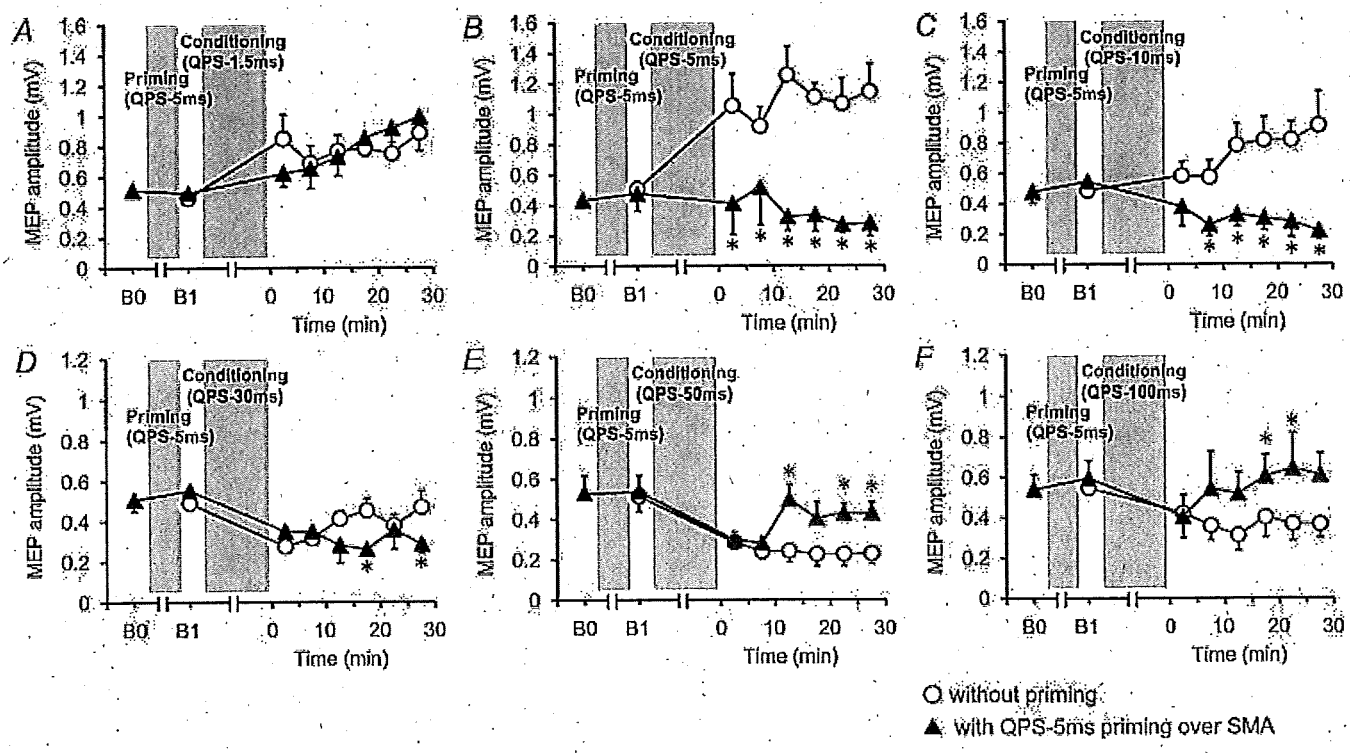

Figure 3. Effects of QPS-5 ms priming over SMA on QPS-induced plasticity
Time courses of MEP amplitude following QPS at various ISIs with (▲) and without (○) QPS-5 ms priming over SMA (mean ± S.E.M.). *A*, SMA priming did not change subsequent LTP-like plasticity induced by QPS-1.5 ms. *B* and *C*, priming reversed MEP sizes induced by QPS-5 ms (*B*) or QPS-10 ms (*C*). *D*, priming enhanced suppression of MEP by QPS-30 ms. *E* and *F*, MEP suppression induced by QPS-50 ms (*E*) and QPS-100 ms (*F*) were not enhanced, but shortened with SMA priming. Asterisks denote significant difference of MEP sizes with priming from those without priming at each time point ($P < 0.05$ by *post hoc* paired *t* tests).

Discussion

We showed that LTD-like and LTP-like QPS-induced plasticity was altered by a preceding period of priming stimulation over SMA. QPS at short ISIs produced an increase in the MEP amplitude, whereas QPS at long ISIs suppressed MEPs (Experiment 1a, Fig. 2*A*). QPS-5 ms priming over SMA occluded MEP facilitation after QPS-5 ms and QPS-10 ms. Furthermore, it enhanced suppression of MEP after QPS-30 ms, but occluded MEP suppression by QPS-50 ms (Experiments 1b, Fig. 5). By contrast, QPS-50 ms priming over SMA inhibited MEP sizes after QPS-5 ms, whereas it facilitated MEP sizes after QPS-30 ms (Experiments 1c, Fig. 5). QPS-5 ms or QPS-50 ms priming over SMA did not change MEP sizes, SICI, ICF and LICI but altered SICF; QPS-5 ms priming enhanced SICF, whereas QPS-50 ms priming erased SICF (Experiment 3, Fig. 7). Finally, a single conditioning TMS over SMA at 110% AMT_{TA} with an ISI of 3 ms significantly inhibited test MEP sizes, whereas no effect was found at a conditioning intensity lower than 110% AMT_{TA}. In addition, no significant effects were found at any conditioning intensity using an ISI of 6 ms (Experiment 4, Fig. 8). We will argue that the present findings provide strong support for the hypothesis that priming over the SMA transiently altered the synaptic efficiencies of excitatory circuits within M1, and that such prior history of neuronal activity alters subsequent LTD-like and LTP-like QPS-induced plasticity through the metaplastic interplay between SMA and M1.

Effects of TMS over SMA

Given that there is now good evidence that TMS can stimulate SMA neurons (Civardi *et al.* 2001; Terao *et al.* 2001; Serrien *et al.* 2002; Verwey *et al.* 2002; Matsunaga *et al.* 2005; Hamada *et al.* 2008*b*), our results are compatible with the idea that rTMS can produce lasting changes in the excitability of these circuits. We argue that such mechanisms underpin the present findings, although we cannot be completely certain about the precise site of our SMA stimulus. According to previous studies, the optimal site of SMA stimulation has been shown to be between 2 and 4 cm anterior to Cz (Terao *et al.* 2001; Serrien *et al.* 2002; Verwey *et al.* 2002); neuroimaging methods also locate the hand area of the SMA proper some 2 to 3 cm anterior to Cz (Hikosaka *et al.* 1996; Lee *et al.* 1999). It is thereby conceivable that our TMS stimulus mainly activates SMA neurons.

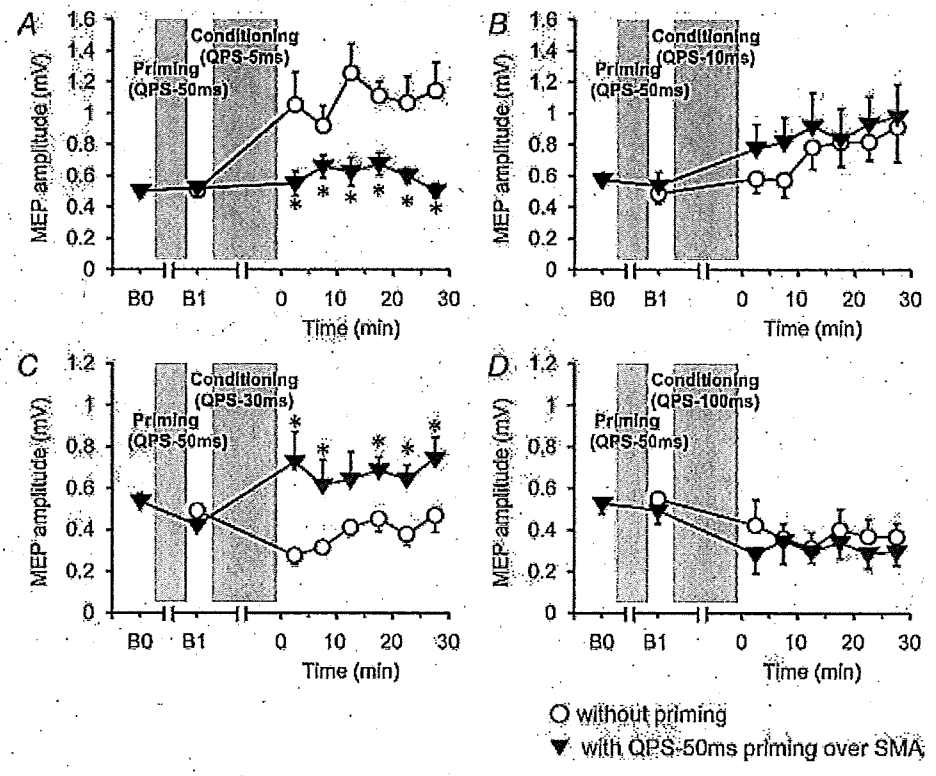

Figure 4. Effects of QPS-50 ms priming over SMA on QPS-induced plasticity
Time courses of MEP amplitude following QPS at various ISIs with (▼) and without (○) QPS-50 ms priming over SMA (mean ± S.E.M.). *A*, SMA priming occluded subsequent LTP-like plasticity induced by QPS-5 ms. *B*, priming did not change plasticity induced by QPS-10 ms. *C*, priming reversed suppression of MEP by QPS-30 ms. *D*, MEP suppression induced by QPS-100 ms was not altered with SMA priming. Asterisks denote significant difference of MEP sizes with priming from those without priming at each time point ($P < 0.05$ by *post hoc* paired *t* tests).

A second question is whether currents induced by stimulation over SMA spread to other motor-related areas. The data suggest that this was unlikely with the intensities of stimulation that we used. Experiment 4a showed that a conditioning pulse over SMA at 110% AMT_{TA} with an ISI of 3 ms significantly inhibited test MEP sizes, which corresponds to the timing of SICI (Kujirai *et al.* 1993), whereas no effect was found at a conditioning intensity of either 70% AMT_{TA} or 90% AMT_{TA}. These findings suggest that the current induced by placing the coil over SMA spreads to $M1_{FDI}$ only when the stimulus intensity is higher than 110% AMT_{TA} in line with a preceding report (Matsunaga *et al.* 2005). In addition, no significant changes in the size of test responses were found at any conditioning intensity using an ISI of 6 ms, which corresponds to the optimal ISI to produce effects in the pathway from PMd to M1 (Civardi *et al.* 2001). Finally, Experiment 4b revealed that no MEPs were elicited during voluntary contraction with single pulse TMS over SMA at very high stimulus intensities up to 100% MSO, indicating no direct activation of excitatory interneurons or cortical output neurons within M1. We cannot completely exclude the possibility that various subliminally stimulated cortical areas including SMA, PMd, PMv, M1 and others regions were implicated in the effects of SMA priming. However, the present findings lead us to conjecture that the effects of priming over SMA can be mainly ascribed to stimulation of the cortex beneath the coil, namely SMA.

Effects of priming over SMA alone

We did not evaluate possible effects of sham priming on subsequent QPS-induced plasticity elicited by all kinds of QPS protocols used in the present paper. In Experiment 2, QPS-10 ms was chosen as a representative of all QPS protocols because it induced mild facilitatory after-effects rendering it more susceptible to possible effects of sham priming. In fact, two control experiments revealed that neither priming alone nor cutaneous sensation had any lasting effect on MEPs.

The results of Experiment 3 show that QPS-5 ms or QPS-50 ms priming over SMA did not change MEP sizes, SICI, ICF and LICI. Its only effect was a transient modulation of SICF, which did not persist as long as the priming effects on QPS. We cannot exclude the possibility that subtle changes in inhibitory circuits were missed because paired-pulse measurements addressing

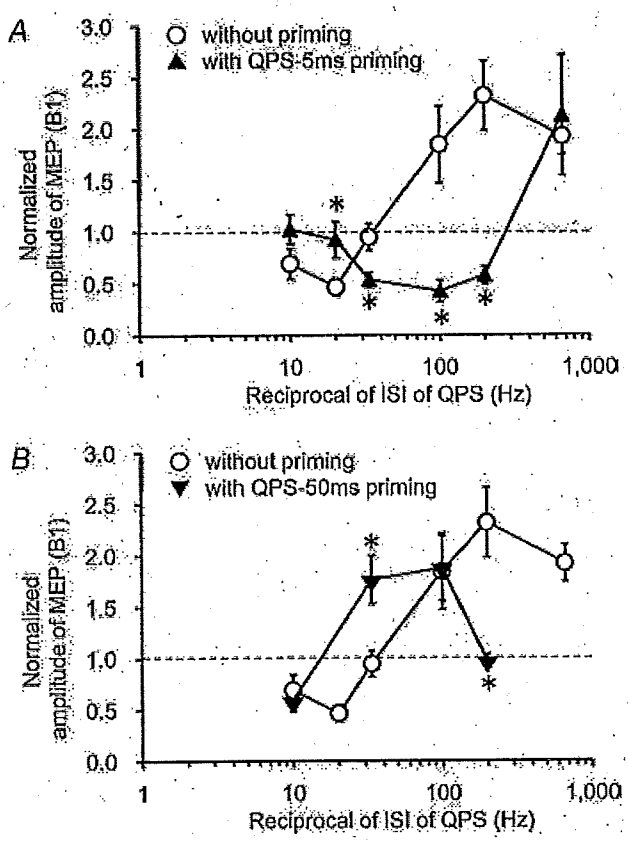

Figure 5. Priming-induced shifts in the stimulus–response function
The normalized amplitudes of MEP at 30 min post conditioning as a function of the reciprocal of ISI of QPS with and without priming over SMA (○). *A*, QPS-5 ms priming (▲). *B*, QPS-50 ms priming (▼). Note that the *x*-axis is logarithmic axis. $^*P < 0.05$ by *post hoc* paired *t* tests.

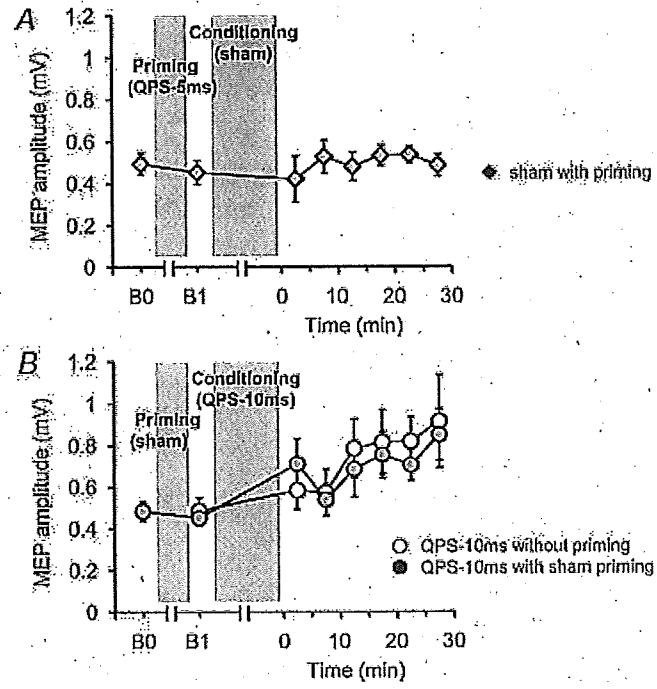

Figure 6. Control experiments
A, sham conditioning with real priming did not modify motor cortical excitability. *B*, the after-effects of QPS-10 ms without priming (open circles) were not different from those of QPS-10 ms with sham priming (grey circles).